

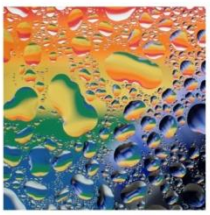

An Assessment of the Mineralogy of UK Municipal Waste Incinerator Bottom Ash using Geochemical Modelling

WRc Ref: UC8564.10
December 2012

An Assessment of the Mineralogy of UK Municipal Waste Incinerator Bottom Ash using Geochemical Modelling

Report No.:	UC8564.10
Date:	December 2012
Authors:	Jane Turrell, Kathy Lewin and Hans van der Sloot (Hans van der Sloot Consultancy)
Project Manager:	Jane Turrell
Project No.:	14728-9
Client:	Environmental Services Association

RESTRICTION: This report has the following limited distribution:

External:	Environmental Services Association

This document has been produced by WRc plc.

Any enquiries relating to this report should be referred to the Project Manager at the following address:

WRc plc,
Frankland Road, Blagrove,
Swindon, Wiltshire, SN5 8YF

Telephone: + 44 (0) 1793 865000
Fax: + 44 (0) 1793 865001
Website: www.wrcplc.co.uk

Contents

List of Tables

List of Figures

Summary

Geochemical modelling of IBA from around the world, including aged IBA samples from the UK, has been undertaken by Hans van der Sloot using LeachXS^{TM}/ORCHESTRA (van der Sloot *et al*, 2008) to support the hazard assessment of IBA currently being undertaken by WRc for ESA. The same modelling has been carried out on data from two fresh samples of IBA collected under the ESA protocol (2010) in December 2010. Key characteristics and model outputs have been placed in context with both UK aged IBA (five samples) and other IBA samples from around the world (six samples) and have shown that total composition, leachability and associated mineralogies are broadly similar.

Excluding the portion of zinc and nickel metal in the samples, the exercise has demonstrated that, at the pH of fresh and aged IBA, the zinc mineralogy that controls release is dominated by zinc silicates ($ZnSiO_3$ or $ZnSiO_4$).

Nickel geochemistry is dominated by the hydroxide. This is exhibited by the two fresh IBA samples, the aged UK IBA samples and the worldwide samples that have been modelled.

Excluding copper metal, copper geochemistry of the aged UK IBA samples and worldwide samples is dominated by copper hydroxide. Calcium copper phosphate hydroxide ($Ca_4Cu(PO_4)_3OH$) and sulphate hydroxides can have a minor role at the lower pH range of aged ashes. In the fresh ashes, copper release is dominated by copper complexed with iron hydroxide and particulate organic matter.

It is recommended that these key phases are used to inform hazard assessment of IBA unless facility-specific geochemical modelling information is available.

1. Aim

This Technical Note presents the results of a geochemical modelling exercise to determine the zinc, nickel and copper species that control observed release in incinerator bottom ash (IBA) using samples taken from two UK municipal waste energy from waste (EfW) facilities.

The work has been completed to inform the understanding of the underlying mineralogy. This is needed to assess specific potentially hazardous properties.

2. Background

Previous discussions between the waste sector and the Environment Agency have focused on the sources of variability in the elemental concentrations of metals in IBA, and the species of metals present, as well as in the sampling methodology. A sampling protocol (ESA, 2010) was agreed with the Environment Agency which aims to provide confidence that sampling and testing is being conducted in a consistent and robust manner.

Zinc, nickel and copper are present in IBA from EfW facilities around the world. Some compounds of these metals carry risk phrases relevant to a hazard assessment and others do not (such as nickel and copper in elemental form). For the purposes of assessing the hazard status of IBA samples, determining which compounds of zinc, nickel and copper control their release is important as only those with relevant risk phrases need to be considered in the assessment of a hazard property[1]. Geochemical modelling provides a means to produce a chemical fingerprint for the speciation of metals in IBA and this technique has already been applied and reported for IBA in other countries and indeed wastes from other treatment processes. IBA from two UK EfW moving grate facilities has been collected for detailed characterisation according to the procedures detailed in the ESA protocol. Geochemical modelling of this data has been used to identify candidate zinc, nickel and copper release controlling species, other than zinc, copper and nickel metal, in the two samples.

[1] Although the term 'risk phrase' is used to describe impacts of exposure to specific compounds at certain concentrations, the term 'hazard classification' is used under the Global Harmonised System, and the regulatory position is currently based on inherent hazard (i.e. the total concentrations of a potentially hazard compound), not on risk of exposure of a target to the hazard.

3. Characterisation

3.1 Methods

Testing was undertaken to determine composition (e.g. acid soluble metals) and release of a many major, minor and trace substances over a wide range of pH conditions and liquid to solid ratios to determine the chemical speciation fingerprint for IBA through geochemical modelling. Besides a selection of possibly relevant mineral phases, reactive Al/Fe oxides and organic carbon fractions were quantified to be support the modelling. The primary tests undertaken included *aqua regia* and hydrofluoric/perchloric acid composition, pH-dependence leaching (CEN/TS 14429:2005) and upflow percolation leaching (CEN/TS 14405:2005). Further background information detailing the basic principles of these tests and the value of the data produced is provided in Appendix A.

3.2 Results

As the geochemical modelling approach has been applied previously to IBA from around the world and to samples of aged UK IBA, key results from the characterisation of the two fresh UK IBA samples have been placed in the context of wider datasets below.

3.2.1 Comparison of UK IBA samples with ESA UK IBA dataset

The 12 month dataset for IBA collected under the ESA IBA sampling and testing protocol (ESA, 2012) has been used to undertake a full 15 hazard property assessment. Key determinands for the assessment have been shown to be acid soluble (total) concentrations of zinc, copper and nickel. These are reported on an 'as received' basis to represent the condition of the ash as it left the EfW facility for treatment and recycling. For most samples this is simply a wet-weight concentration, with others including a calculation of any inert non-grindable materials (ceramics, glass, stone) removed during the sample preparation stage. The concentrations of the three key metals for the two fresh UK IBA samples are compared with the ESA UK dataset in Table 3.1.

Table 3.1 'As received' concentrations of key metals in the two UK IBA samples and ESA UK IBA dataset used for hazard assessment

Metal	UK IBA1	UK IBA2	ESA UK IBA dataset (Jan-Dec 2011)*		
			Average	95%ile	Maximum
Zn mg/kg**	2514	1963	2107	3292	9389
Ni mg/kg	94.0	50.1	135	420	1050
Cu mg/kg**	3940	3942	1900	3679	17871

Notes:

*411 samples

**Zn and Cu determinations undertaken on 11 replicate acid digestions and the average reported as per the ESA IBA protocol (2010).

For both samples nickel concentrations were below the average concentration for the ESA dataset, and copper concentrations exceeded the 95th percentile concentrations for the ESA dataset. The UKIBA1 zinc concentration was between the average and 95th percentile concentration, while UKIBA2 was below the average concentration. No determinand in the fresh IBA was therefore at extreme concentrations for the UK IBA dataset.

3.2.2 Comparison of unprocessed and processed UK IBA data

Data for 'fresh' IBA samples collected from two UK EfW facilities in December 2010 has been compared with geochemical data for aged, processed UK IBA (Appendix B). The study on processed IBA of varying ages was commissioned by Ballast Phoenix Ltd in 2006 in which five samples were taken at separate Ballast Phoenix reprocessing facilities.

The plots reproduced in Appendix B indicate that the new and historic pH dependence and upflow percolation leaching data are comparable. These plots demonstrate that the leaching behaviour of fresh and aged IBA are very similar under the same pH conditions and liquid to solid ratios. This represents an important finding with respect to demonstrating that the characteristics of fresh and aged IBA from the UK is similar in terms of the mineralogy that is controlling metal release. The plots show that there is consistency in the leachability of two fresh and 5 aged samples of UK IBA over time (a four year period) and more importantly that the behaviour of fresh and processed IBA is also comparable.

3.2.3 Comparison of UK IBA with world-wide data

A comparison of leachability data has been undertaken between the two UK bottom ashes studied in this work with municipal waste IBA of worldwide origin (Appendix C). Data from a total of 13 facilities (12 moving grate and one rotary kiln) has been compared with UKIBA1 and UKIBA2.

The data indicates there are no substantial differences in the leaching behaviour of metal and other key parameters between the UK and global data set which includes both fresh and aged IBA.

As the leaching behaviour of IBA is the result of the underlying mineralogy, sorption reactions and substitution reactions we would expect IBA produced by municipal EfW facilities around the world to have a consistent mineralogical fingerprint with respect to metals.

3.3 Geochemical speciation modelling of IBA

Geochemical modelling of the metal species in IBA has been conducted by Hans van der Sloot (formerly of ECN, Energy research Centre of the Netherlands) on IBA from around the world using LeachXS^{TM}/ORCHESTRA. The geochemical modelling of the two composite samples of fresh IBA from the UK, referred to as UKIBA1 and UKIBA2, is therefore reported in the context of the wider work.

A resumé of the geochemical modelling work and plots to illustrate model outcomes are provided in Appendix D1. Multi-element geochemical speciation modelling is equilibrium based and complex due to the multiple simultaneous interactions between major, minor and trace elements (e.g. mineral dissolution/precipitation, competition for sorption sites on hydrated iron oxides and organic matter and substitution in solid solutions). Model run-times are short and the outcomes of the model can be optimized by iteration and by applying changes in the 'proposed' mineral assemblage until simultaneously a good match is obtained simultaneously between modelled mineral assemblage (and sorption sites) and actual data for all major, minor and trace elements. The emphasis in this type of modelling is focused on the concentrations in solution in contact with the solid phase. It therefore provides information about the solubility controlling phases in the ash. The options to vary mineral selections is very limited as a good agreement between all major, minor and trace elements is required. Focusing on a single substance may produce a good fit for one, but a very poor match for other substances. Incorrect choices of a mineral or a sorption property will show as a significant deviation of predicted leaching from actual measurement i.e. a "poor fit". Example of "good" and "poor fits" for the modelling are presented in Figures 3.1 and 3.2. The model results from Figure 3.2 indicate that ZnO or $Zn(OH)_2$ are not controlling solubility indicating that these phases are not in play.

Figure 3.1 Example of a "good fit" - $Zn(SiO_3)$ in UKIBA1

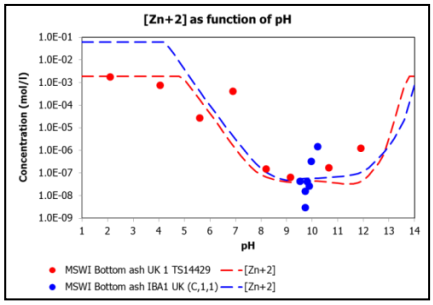

Figure 3.2 Examples of "poor fit" – ZnO in UKIBA1 and $Zn(OH)_2$ in UKIBA2

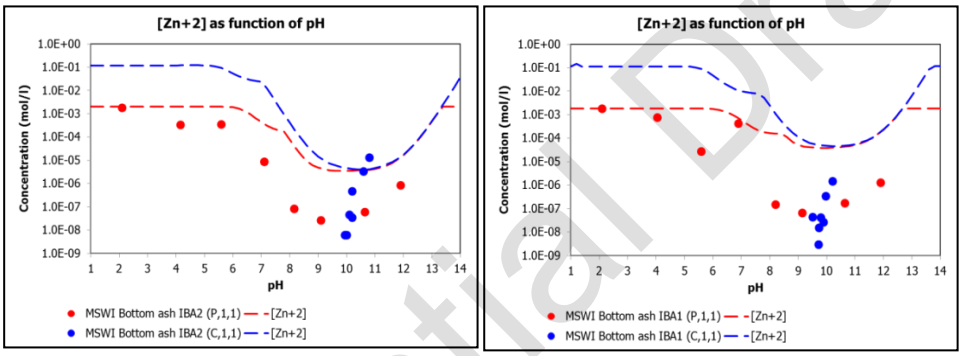

The modelling approach used in this instance takes into account partitioning between the dissolved (free and bound to dissolved organic carbon (DOC)) and solid phases (iron and aluminium oxide/hydroxide sorption and clay sorption properties of the material) to determine the major mineral phases present for each element which are controlling observed leaching characteristics. Mineral phases are initially selected on the basis of saturation indices (where 0 represents full equilibrium, negative values represent under-saturation and positive values represent oversaturation) at various pH conditions. A model outcome close to zero over a broad pH range would indicate that the mineral phase is a good match and likely to be a controlling phase for observed leaching characteristics. This initial set of possible controlling minerals is then optimized to obtain a full description of the release at L/S=10 for all major, minor and trace elements, which is then verified against the measurements at low L/S (first fraction of the percolation test) by modelling simultaneously the concentrations in solution at a L/S of 0.3. Modelling of multiple IBA samples from different sources leads to largely the same mineral set, which provides an adequate description indicating that IBA processed in incinerators produce an ash with very similar properties from a leaching perspective. An example of a full elemental fit with associated partitioning is provided in Appendix F.

The plots showing dominant solid phases for the best fit mineral assemblages are presented in Appendix F for the UK and world-wide dataset. It should be noted that the presence of elemental or metallic nickel, copper and zinc are not included in the modelling.

3.3.1 Geochemical speciation modelling IBA

Any of the modelling described below for the individual elements zinc, nickel and copper is based on full multi-element geochemical modelling with variations in the mineral assemblage to test the stability of the selected mineral set.

Zinc

Zinc has been selected as the parameter to demonstrate the outcome of the geochemical modelling of IBA from around the world, including aged UK samples and the fresh IBA tested for ESA. Between these ashes zinc exhibits solubility control by a few poorly soluble phases.

In an environmental situation the pH domain of relevance is defined by the initial pH of the bottom ash (around pH 12) and a fully carbonated bottom ash (pH around 7.5). The plots showing dominant phases for the best fit mineral assemblages are presented in Appendix F1 for the UK and world-wide dataset. Plots for solid phase fractionation only are presented in Appendix F2. It should be noted that the modelling does not take into account the presence of metallic or elemental zinc in the IBA although this will most likely be present in the sample. The optimal release match ('best fit') was achieved for all 12 samples by either of these poorly soluble mineral phases, in addition to organic matter interaction and sorption on iron oxide/hydroxide surfaces:

- a silicate: $ZnSiO_3$ (or $ZnSiO_4$, willemite); or
- a calcium zinc phosphate hydroxide: $Ca_4Zn(PO_4)_3OH$.

The plots show that the release controlling phases for zinc will be these mineral forms at the natural pH of the ash.

Reiteration of the modelling with refinements of the mineral suite has shown that the two fresh samples are controlled by zinc silicate across the pH domain of both fresh and aged ash in most scenarios. In some combinations of mineral assemblage, calcium zinc phosphate hydroxide can play a role between pH 9 and 5.5. However, this is the pH domain of aged ashes and the modelling of actual aged ashes indicates a predominance of the silicate at this pH range.

Separate model runs were carried out for a range of other minerals as single controlling phases. A poor match with measured concentrations for the fresh ashes was obtained for ZnO, cazincate, $Zn(OH)_2$, willemite ($ZnSiO_4$), $ZnCl_2$ and bianchite ($Zn_{0.75}Fe^{2+}_{0.25}(SO_4)\bullet 6(H_2O)$). This implies that the latter phases are not the phases controlling leaching over the pH range of relevance to IBA in normal exposure conditions, or in fresh ash as it leaves the facility. Any soluble zinc will dissolve and more or less immediately re-precipitate as the less soluble silicates and phosphates – as would happen when the ash is quenched as it comes out of the boiler.

Silicates ($ZnSiO_3$ and willemite, $ZnSiO_4$) or phosphate hydroxides have therefore been shown to control the release of zinc across the pH domain of both fresh and aged samples in the UK and around the world, supporting the view that IBA is a generic waste with respect to the underlying zinc mineralogy that controls its release.

Comparison of the *aqua regia* zinc concentration in UKIBA1 and 2 with the ESA IBA dataset (Table 1) shows that the samples are close to the average concentration for the ESA dataset. The outcome of the modelling is therefore considered to be applicable to the assessment of hazard status of the ESA dataset.

Nickel

A similar modelling exercise has been undertaken for nickel species, including modelling runs of different mineral assemblages to test the fit of the predicted and actual measurements. The plots are presented in Appendix F3. However, as fractionation in the solid phase is of greatest interest, plots demonstrating fit, liquid to solid partitioning and fractionation in solution are not reproduced here. The plots for the two fresh UK IBA samples are presented in Figure 3.3.

Figure 3.3 Plots showing the geochemical modelling of solid phase fractionation of IBA for nickel (full plots in Appendix F4)

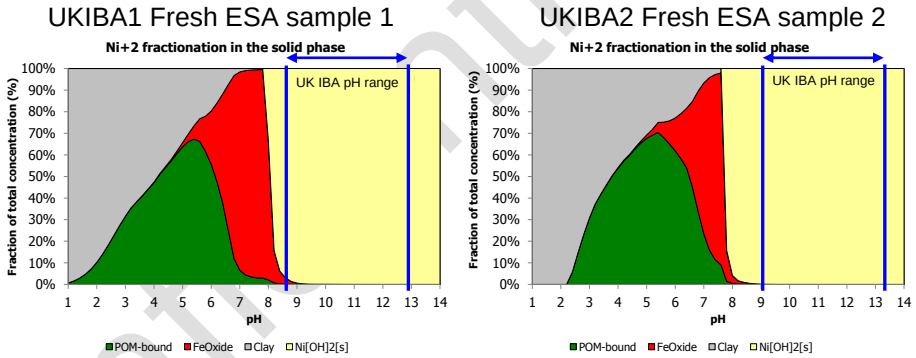

The plots indicate that the mineralogy that controls the release of nickel above pH 8 is dominated by nickel hydroxide. These plots are very similar to those for the aged IBA and for IBA from around the world as shown in Appendix F4. Therefore within the normal pH conditions of fresh and aged IBA, nickel hydroxide is dominant, supporting the hypothesis that IBA can be considered to be a generic waste stream with respect to the geochemistry of nickel. This assessment excludes the portion of the nickel concentration that is attributable to nickel metal in the sample.

Copper

The modelling has been repeated for copper species, including modelling runs of different mineral assemblages to test the fit of the predicted and actual measurements. Unlike most

other elements a number of reiterations using different mineral assemblage have been required to improve the modelling fit for the fresh UK ashes. The plots showing fractionation in the solid phase are presented in Appendix F3.

The picture for copper is less obviously consistent than for nickel.

- Aged ashes: examination of the plots for aged ash from UK and around the world, shows that the major controlling phase at high pH (>pH12) in aged samples is copper hydroxide. In some model iterations (not shown) under the pH domain of aged ashes (<pH10) phosphate hydroxide could be a minor phase for copper release, with copper hydroxide representing a transient phase before pH reduces during the carbonation process. In the worldwide samples copper hydroxide dominates copper release at high and moderate pH values, although copper sulphate hydroxides (e.g. tsumebite and anterlite) may play a role as the pH decreases (Appendix F3).

- Fresh ashes: following the repeated modelling iterations, a different picture has emerged for the fresh IBA samples, where copper release is dominated by copper complexed with particulate organic matter bound copper and iron hydroxide. The role of organic matter in the release of copper has been widely reported (e.g. van Zomeren and Coumans, 2004), but the levels of available organic matter are higher in the UK fresh ashes than previously modelled (i.e. in aged IBA). The characterisation exercise for the UK fresh ashes (WRc, 2010) demonstrated that these samples still contained relatively high levels of organic matter (e.g. up to 2900 mg/kg organic hydrophyllic acids). These are normally microbially degraded or washed out during IBA treatment or rainfall exposure. The modelling therefore shows that in very fresh ashes which still contain available organic matter, the phases controlling release of copper are iron hydroxide and particulate organic matter.

The modelling exercise has highlighted that the ash ageing process represents a continuum until full carbonation of the IBA at pH 7-8 over decades. It is understood that in the early stages of this process, at the same time that organic matter is gradually removed, copper hydroxide is formed as part of secondary mineralisation and is repeatedly precipitated as a coating on inorganic particles. This secondary mineralisation increases the dominance of copper hydroxide with time, followed by the conversion to other inorganic phases, depending on the availability of other ions, e.g. phosphate hydroxides or sulphate hydroxides and over many decades, carbonates.

However, it should be noted that copper metal is easily brought into solution by *aqua regia* digestion and therefore a significant but unquantifiable component of the IBA is likely to be copper metal (e.g. copper wire), in addition to the mineral phases modelled from the leachability and composition data. Anecdotal evidence from ash reprocessors that recover and sell ferrous and non-ferrous metals indicates that, of the baseload of 2000 mg/kg Cu in IBA (average concentration for the ESA dataset, Table 3.1), up to 1000 mg/kg is likely to represent metallic copper. Similarly, excursions above this value (e.g. values of 3000, 5000 or

10000 mg/kg) almost certainly represent copper metal fragments, such as e.g. copper wire (van der Sloot, *pers. comm.)* or alloys such as brass. However, these non-hazardous forms are indistinguishable from other copper phases dissolved in the *aqua regia* digest. The assessment of the copper controlling phases is therefore conservative as it makes no allowance for the metallic copper in IBA.

Comparison of the *aqua regia* copper concentrations in UK IBA1 and 2 with the ESA IBA dataset (Table 1) shows that the fresh samples are slightly higher than the 95%ile concentration for the ESA dataset (3679 mg kg^{-1}). The outcome of the modelling of copper speciation is therefore considered to be applicable to the assessment of hazard status of the ESA dataset, but can be over-ridden by facility-specific modelling.

4. Conclusions

1. Two samples of fresh IBA have been collected in line with the ESA IBA protocol, characterised with respect to composition and leaching behaviour and geochemical fingerprints by multi-element modelling for zinc, copper and nickel species have been generated using LeachXS^{TM}/ORCHESTRA.

2. The characteristics of the two fresh IBA samples, UK IBA1 and UK IBA2, fall within the ranges exhibited by the ESA IBA dataset January-December 2011, which has been used as the basis of a 15 property hazard assessment (ESA, 2012).

3. The leaching behaviour of the two fresh IBA samples with respect to zinc, copper and nickel is similar to that exhibited by five UK aged IBA samples and a further five samples from around the world.

4. Geochemical modelling shows that a small number of mineral phases control the speciation of zinc, copper and nickel across the majority of samples in the pH domain of fresh and aged IBA (pH9-13).

5. The dominant zinc controlling phases for the UK IBA samples modelled are silicates ($ZnSiO_3$ or $ZnSiO_4$). Modelling of the 12 samples from the UK and around the world indicate that either silicates or phosphate hydroxides control zinc release pointing to an underlying consistent mineralogy.

6. Within the normal pH conditions of fresh and aged IBA, the release of nickel is dominated by nickel hydroxide. This is the case for the worldwide samples, the aged UK IBA and fresh UKIBA, indicating the generic nature of nickel geochemistry in IBA

7. The modelling has indicated that copper release from the two UK samples of fresh IBA is dominated by copper complexed with iron oxide and particulate organic matter, whereas copper hydroxide and hydroxide phosphates dominate the release from aged samples. The secondary mineralisation of the sample with respect to copper hydroxide precipitation occurs as the particulate organic matter is degraded or washed away. The modelling highlights the continuing ageing process from the formation of very fresh ash that still contains relatively high levels of hydrophyllic organic acids, through to full carbonation, which will take decades, In addition to these phases a high portion of the total copper, not accounted for in the modelling, is attributable to non-hazardous copper metal fragments, which is highly soluble in the *aqua regia* used to digest the samples. It should also be noted that the proportion of metallic copper dissolved in the aqua regia (e.g. copper wire) is indistinguishable to the copper that is present in inorganic phases, and is also not accounted for in the geochemical modelling. The average concentration of Cu in the ESA dataset is 2000 mg/kg. Anecdotal evidence

indicates that 1000 mg/kg probably represents metallic copper. Similarly, excursions above 2000 mg/kg almost certainly represent metal fragments, e.g. copper wire. The assessment of the copper controlling phases is therefore conservative as it makes no allowance for the metallic copper in IBA.

8. We conclude that the speciation of zinc, copper and nickel in IBA is not specific to a particular facility but is controlled by the overall conditions present in a high temperature oxygenated thermal treatment process.

9. It is recommended that these key phases are used to inform hazard assessment of IBA from unless facility-specific geochemical modelling information is available.

References

ESA (2010) A sampling and testing protocol for the assessment of hazard status of incinerator bottom ash. Environmental Services Association (2010)

Environment Agency (2011) Technical Guidance WM2 – Hazardous Waste: Interpretation of the definition and classification of hazardous waste v2.3.
http://www.environment-agency.gov.uk/business/topics/waste/32200.aspx

CEN/TS 14405 (2004): Characterization of waste - Leaching behaviour tests - Up-flow percolation test (under specified conditions), CEN, Brussels, Belgium.

CEN/TS 14429 (2005). Characterization of waste - Leaching behaviour tests - Influence of pH on leaching with initial acid/base addition, CEN, Brussels, Belgium.

Garrabrants, A.C., Kosson, D.S., van der Sloot, H.A., Sanchez, F. and Hjelmar, O. (2010). "Background Information for the Leaching Environmental Assessment Framework (LEAF) Test Methods" USEPA, EPA/600/R-10/170.Preliminary EPA Method 1313 (2009) - Leaching test (liquid-solid partitioning as a function of extract pH) of inorganic species in solid materials using a parallel batch extraction test. US Environmental Protection Agency, 2009.

van der Sloot, H.A., Seignette, P.F.A.B., Meeussen, J.C.L., Hjelmar, O. and Kosson, D.S. (2008). A database, speciation modelling and decision support tool for soil, sludge, sediments, wastes and construction products: LeachXS™- Orchestra. In: Second international symposium on energy from biomass and waste, Venice 2008.

WRc (2011). IBA characterisation data to support geochemical modelling. Analysis report UC8547-draft March 2011. Kathy Lewin, Jane Turrell, James Peacock, Victoria Benson and Andre van Zomeren. WRc, 2011a. Statement to support the classification of IBA as non-hazardous waste.

WRc (2012) Assessment of hazard classification of UK IBA Report for the January-December 2011 IBA dataset : UC8540.09 October 2012. Draft.

Appendix A Background Information on Waste Characterisation Tests

A1 pH-dependence leaching test

The pH-static test (CEN/TS 14429, 2005) was used to characterise the pH dependent leaching behaviour of size reduced stabilized waste. In short, this leaching test involves leaching the crushed material at eight pH values ranging from pH 2 to 13, each at a liquid to solid ratio (L/S) of 10. HNO_3 (10 M) and NaOH (10 M) were used to adjust the pH to the desired value. The pH was checked and adjusted accordingly after 6 hours of equilibration. After 48 hours, the final pH and electrical conductivity (EC) was measured, and the eluates were filtered (0.45 µm) and analysed.

A2 Percolation test

The percolation test on the size reduced material (95% < 4 mm) was carried out according to CEN/TS 14405:2004. In this column test 7 eluate fractions were collected within the range of L/S = 0.1-10 l/kg. The total test duration was approximately 21 days. The leachant was demineralised water (DMW). The test material was leached in a column operated in up-flow mode (14 ml/h) using a column height of 30 cm and a diameter of 5 cm. The eluates were filtered through 0.45 µm membrane filters and analysed.

A3 Chemical analysis

The eluates from the laboratory tests were analysed for major, minor and trace elements using ICP-AES, for DOC using a Shimadzu 5000-a TOC analyser, for anions using ion-chromatography and for cyanides (total and free) using photometry.

A4 Test data presentation

The characterisation of the leaching behaviour of materials like IBA is best carried out by a combination of the pH dependence leaching test (CEN/TS 14429), and a percolation test (CEN/TS 14405), as this combination allows many conclusions on release behaviour to be drawn (including the long term and after full disintegration). It also provides a reference base for comparison with any type of other leaching test. Plots are presented in the following Appendices, with explanation in the first section of each. Note: the repeatability in the test data is good for both leaching test methods[2] and we can be confident in these comparisons.

[2] A partial validation of both methods is ongoing in parallel with the validation of draft EPA methods 1313 and 1314 (6. Garrabrants, A.C., Kosson, D.S., van der Sloot, H.A., Sanchez, F., and Hjelmar, O., 2010. "Background Information for the Leaching Environmental Assessment Framework (LEAF) Test Methods" USEPA, EPA/600/R-10/170.).

Appendix B Leaching Test Data in Context of Dataset for UK Aged IBA

In this Appendix leaching data is compared with the UK dataset for incinerator bottom ash generated in 2006. Data from the pH dependence test (CEN/TS14429), and the upflow percolation test (CEN/TS14405) are shown.

It can be seen that all the data from the two bottom ash samples tested (labelled here MBA UK1 and MBA UK2) were within the 90% confidence limits for the worldwide data, and generally showed good agreement with the average. The graph of cumulative release versus L/S allows conclusions on the main release mechanism. If a slope of one is observed, release is controlled by solubility limitations. If the release curve is horizontal (= no further release with increasing L/S), this points to depletion of a fully dissolved species (e.g. Cl).

For the pH dependence plot, the range that is relevant for what species are present in the IBA are between the natural pH of the IBA (pH 11-12) and pH of fully carbonated IBA (pH 7.5).

Figure B.1 Cumulative and pH dependent release for selected parameters

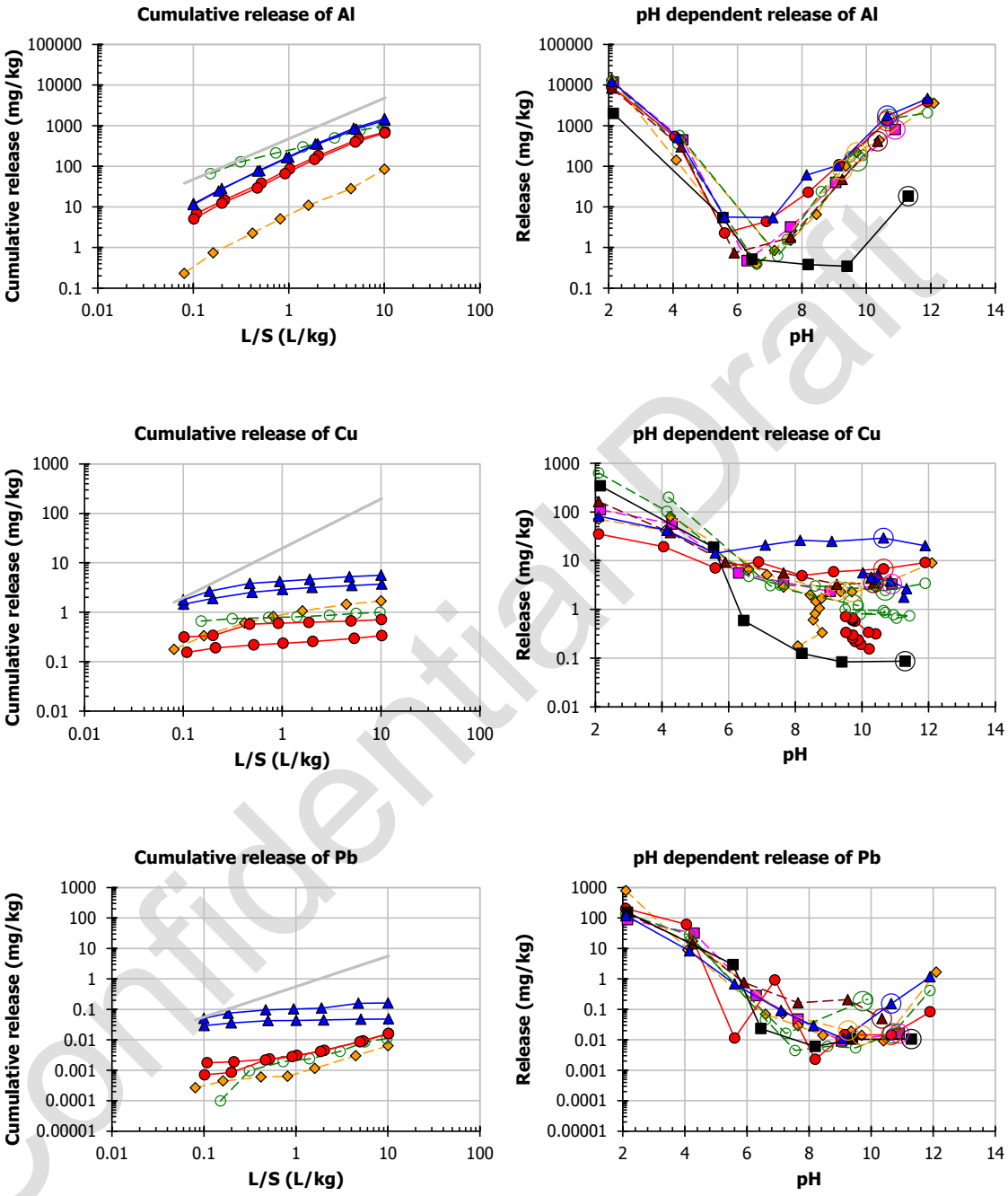

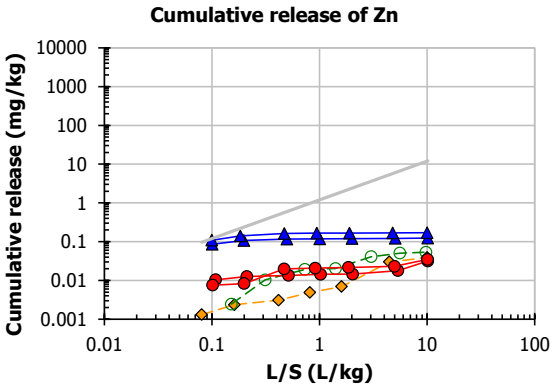

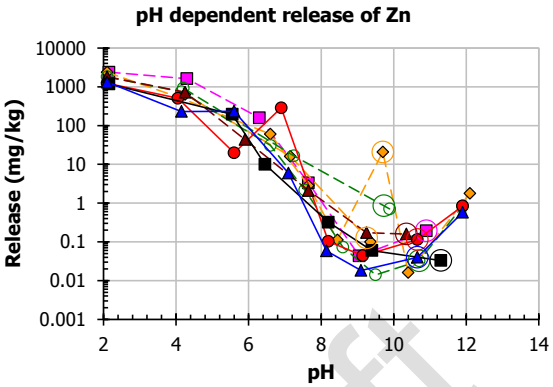

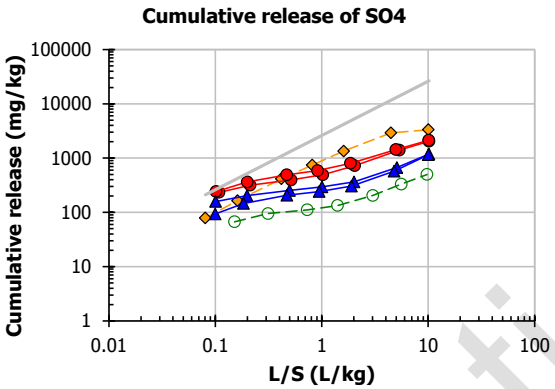

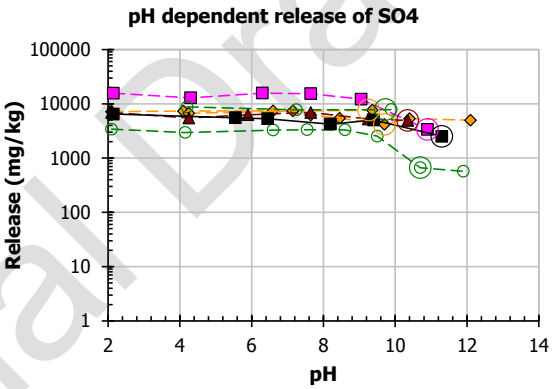

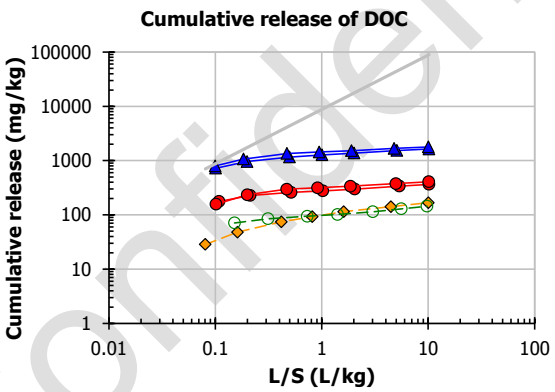

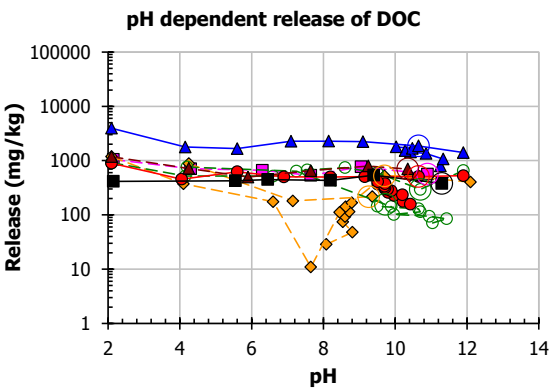

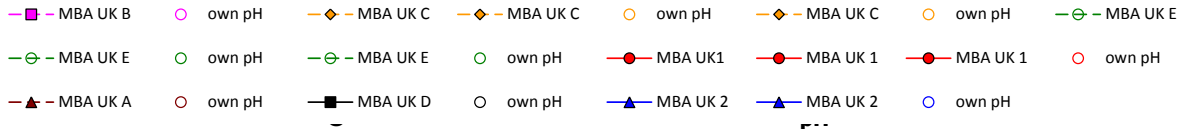

Appendix C Leaching Test Data in Context of Worldwide Dataset

In this Appendix leaching data is compared with the worldwide dataset for incinerator bottom ash. Data from the pH dependence test are shown on the left (TS14429), with the upflow percolation test data across varying liquid to solid ratios shown on the right (TS14405).

The average for all data is shown by the black dashed line, with the upper and lower 90% confidence intervals shown by the grey dashed lines.

It can be seen that all the data from the two bottom ash samples tested were within the 90% confidence limits for the worldwide data, and generally showed good agreement with the average.

Note: in the following appendices the labels MBA UK1 and MBA UK2 refer to samples UK IBA1 and UK IBA2

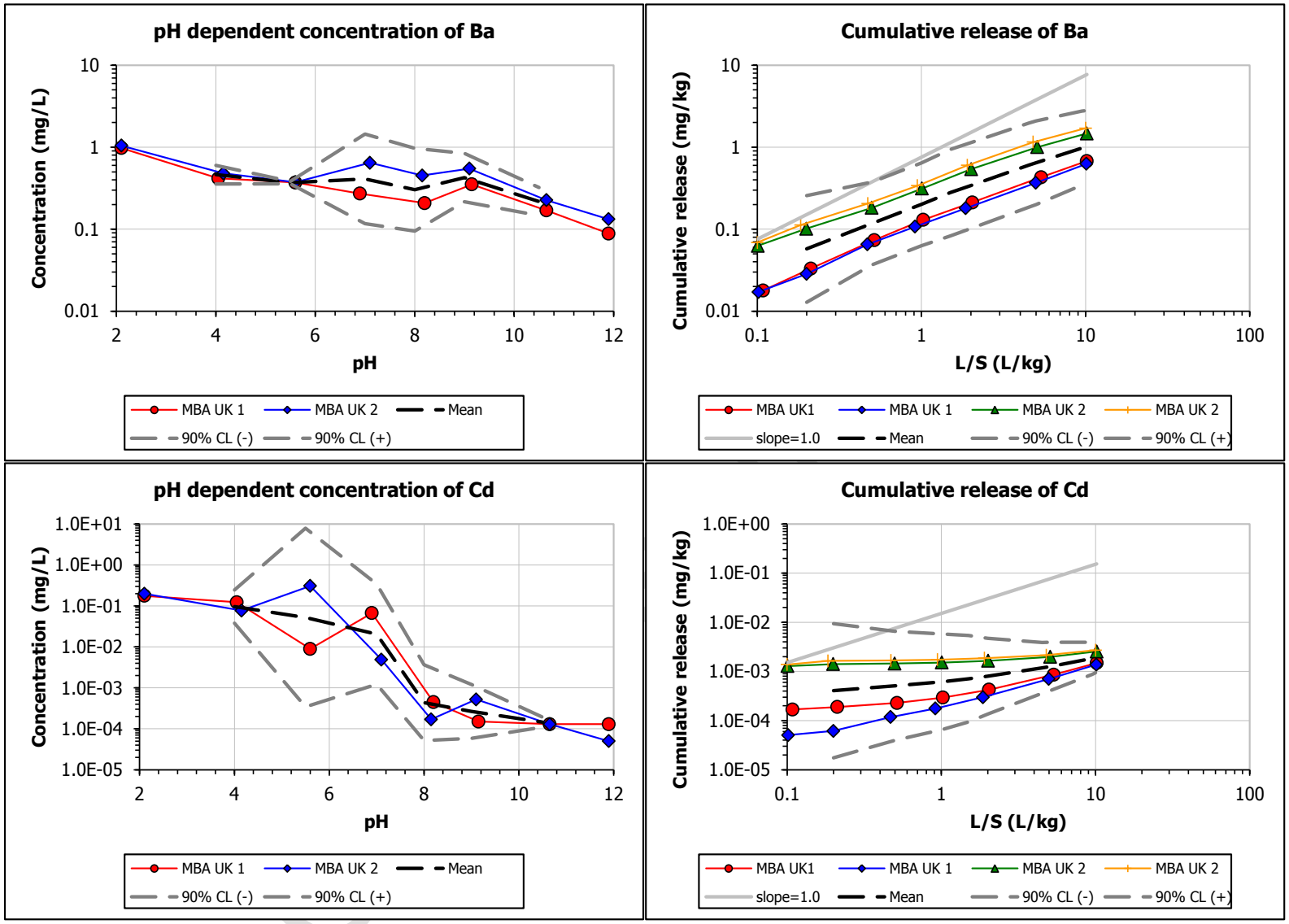
pH dependent concentration of Ba
Concentration (mg/L)
10
1
0.1
0.01
2
4
6
8
10
12
pH
MBA UK 1
MBA UK 2
Mean
90% CL (-)
90% CL (+)
Cumulative release of Ba
Cumulative release (mg/kg)
10
1
0.1
0.01
0.1
1
10
100
L/S (L/kg)
MBA UK1
MBA UK 1
MBA UK 2
MBA UK 2
slope=1.0
Mean
90% CL (-)
90% CL (+)
pH dependent concentration of Cd
Concentration (mg/L)
1.0E+01
1.0E+00
1.0E-01
1.0E-02
1.0E-03
1.0E-04
1.0E-05
2
4
6
8
10
12
pH
MBA UK 1
MBA UK 2
Mean
90% CL (-)
90% CL (+)
Cumulative release of Cd
Cumulative release (mg/kg)
1.0E+00
1.0E-01
1.0E-02
1.0E-03
1.0E-04
1.0E-05
0.1
1
10
100
L/S (L/kg)
MBA UK1
MBA UK 1
MBA UK 2
MBA UK 2
slope=1.0
Mean
90% CL (-)
90% CL (+)

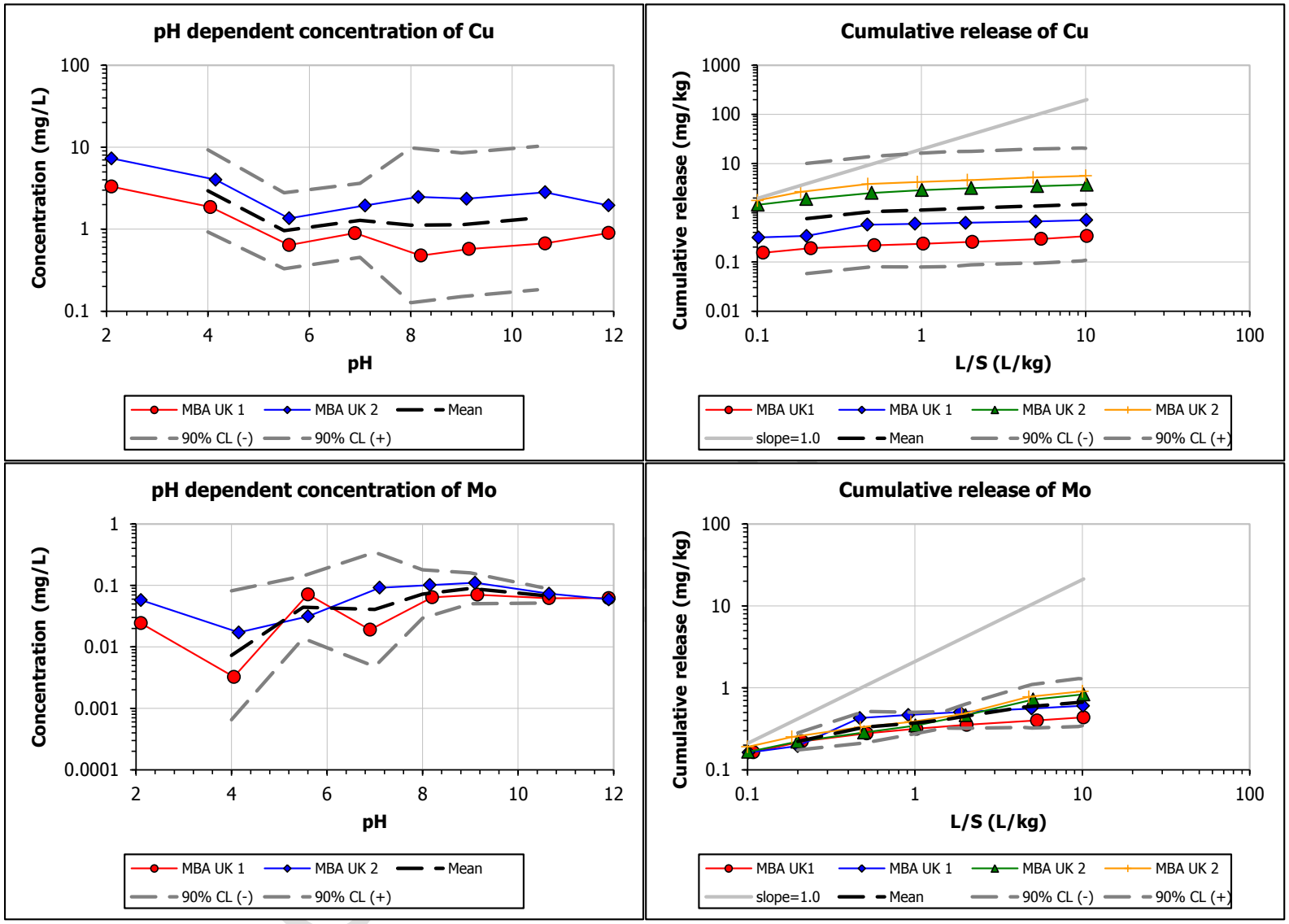
pH dependent concentration of Cu
Concentration (mg/L)
100
10
1
0.1
2
4
6
8
10
12
pH
MBA UK 1
MBA UK 2
Mean
90% CL (-)
90% CL (+)
Cumulative release of Cu
Cumulative release (mg/kg)
1000
100
10
1
0.1
0.01
0.1
1
10
100
L/S (L/kg)
MBA UK1
MBA UK 1
MBA UK 2
MBA UK 2
slope=1.0
Mean
90% CL (-)
90% CL (+)
pH dependent concentration of Mo
Concentration (mg/L)
1
0.1
0.01
0.001
0.0001
2
4
6
8
10
12
pH
MBA UK 1
MBA UK 2
Mean
90% CL (-)
90% CL (+)
Cumulative release of Mo
Cumulative release (mg/kg)
100
10
1
0.1
0.1
1
10
100
L/S (L/kg)
MBA UK1
MBA UK 1
MBA UK 2
MBA UK 2
slope=1.0
Mean
90% CL (-)
90% CL (+)

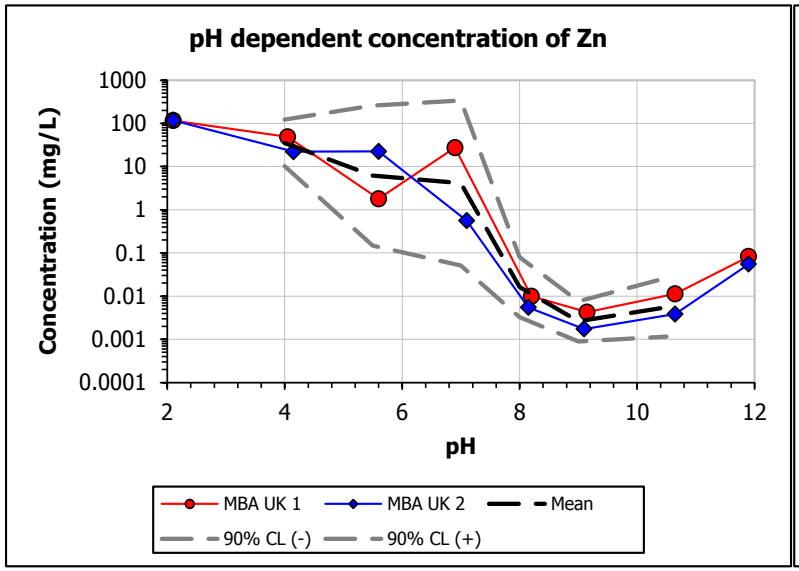

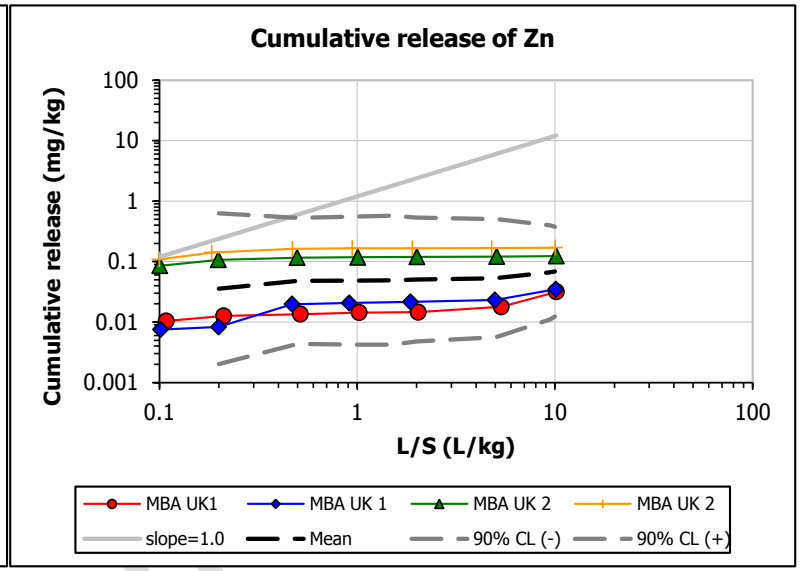

Appendix D Geochemical Speciation Modelling of IBA Generated Using Zinc as Example Species

Chemical speciation of the eluates obtained from the pH dependence (CEN/TS14429) and percolation leaching test (CEN/TS14405) carried out on IBA1 and IBA2 was calculated using the ORCHESTRA modelling framework (Meeussen, 2003). Aqueous speciation reactions and selected mineral precipitates were taken from the MINTEQA2 database. Ion adsorption onto organic matter was calculated with the NICA-Donnan model (Kinniburgh *et al.*, 1999), with the generic adsorption reactions as published by Milne *et al.* (Milne *et al.*, 2001; Milne *et al.*, 2003). Adsorption of ions onto iron and aluminium oxides was modelled according to the generalized two layer model of Dzombak and Morel (Dzombak and Morel, 1990).

The database/expert system LeachXS™ (www.leachxs.net) was used for data management and for visualization of the calculated and measured results (van der Sloot *et al.*, 2001; van der Sloot *et al*., 2003; van der Sloot *et al*., 2007; van der Sloot *et al.*, 2008). The coupled LEACHXS - ORCHESTRA combination allows for very quick data retrieval, automatic input generation for modelling, processing of calculated results and graphical and tabular data presentation.

The input to the model consists of metal availabilities, selected possible solubility controlling minerals, active Fe-and Al-oxide sites (Fe- and Al-oxides were summed and used as input for hydrous ferrous oxide (HFO) as described by Meima and Comans (Meima and Comans, 1998)), particulate organic matter and a description of the DOC concentration as a function of pH (polynomial curve fitting procedure). The DOC analysis of the extracts does not represent the reactive part of the dissolved organic matter. Based on experience with other similar samples, where the quantification between hydrophilic, fulvic and humic acid fraction in DOC has been quantified, reactive fractions of DOC are defined as a function of pH (lowest proportion of reactive forms at neutral pH and increasing towards both low and high pH (van Zomeren and Comans, 2007)). A polynomial fit is created through the eight data points to allow quantification of the reactive DOC at intermediate pH values in modelling. Basically, the speciation of all elements is calculated using a single problem definition in the model with the same parameter settings. This limits the degrees of freedom in selected parameter settings considerably, as improvement of the model description for one element may worsen the outcome for other elements. The maximum value as obtained in the pH dependence leaching test (between pH 3 and 13) was used as the available concentration. Total inorganic carbon (TIC) in eluate is not a good measure for the actual carbonate level as upon acidification carbonate is lost from solution as CO_2. This means that TIC (recalculated as carbonate) in the solid must be taken as the available quantity.

The mineral phases that were allowed to precipitate were selected after calculation of their respective Saturation Indices (SI) in the original pH dependence leaching test eluates.

Saturation indices were calculated for all > 650 minerals in the thermodynamic database and a selection of the most likely and relevant phases was made based on the degree of fit over a wide pH range and the closeness of the SI value to 0 and an expert judgment on suitability of possible minerals for the waste mixture (e.g. exclusion of high temperature minerals). Generally, minerals were selected if the SI was in the range of -0.2 to 0.2 for more than two pH data points. Since the SI calculation does not take competition between substances for the same sorption sites into account, sometimes phases prove to be relevant that do not seem relevant from an SI calculation. In addition, phases may appear relevant based on SI calculation, but are of no relevance due to the slow kinetics of dissolution (Nordstrom, 2009). This relates in particular to several clay minerals and rock phases. Finally, it should be realised that there is a significant difference between minerals identified by XRD on bulk samples and the mineral and sorptive phases controlling leachability. The latter are sometimes minor quantities present as coatings on particles.

The model results for the MSW IBA, compared with the original pH dependence test data, are provided in Appendix E. In all cases, the percolation test data are given for comparison, as the modelling is carried out with the same parameter settings both at L/S=10 and at L/S around 0.2 to assess the validity of the mineral and sorption parameter selection for both a wide pH range as well as a wide L/S range.

The starting point for the modelling is the L/S=10 leach test dataset. The optimization of the mineral selection is based on obtaining a prediction that provides the closest fit between model and actual test results. The low L/S modelling (around 0.2) using the first fraction of the percolation test, is meant to test whether the same selection of minerals or a slight modification can simultaneously predict the release behaviour at low L/S under the assumption that local equilibrium prevails.

Based on the preliminary model run to determine SI values, expert knowledge (relevant mineral phases formed under ambient conditions) a preliminary set of minerals is identified to run the model. Based on a criterion of less than 1‰ of the element present in a given mineral phase, the selection of relevant minerals can be narrowed down.

Some 25 elements are taken along in the chemical speciation modelling for the MSWI bottom ashes. The input parameters for the modelling are given in Tables D1 and D2 for IBA1 and IBA2 respectively. These comprise the element availabilities, the mineral selection, the content of clay to the extent relevant, the quantity of reactive Fe- and Al- oxide surfaces and the reactive part of particulate and dissolved organic matter. The selection of minerals for the calculation run is wider than the actual minerals found to be of relevance. The material properties in terms of element availabilities, Fe- and Al-oxide quantity, clay content, relevant minerals and reactive particulate (designated as solid humic acid - SHA) and dissolved organic matter (designated as dissolved humic acid DHA) form a chemical speciation fingerprint (CSF) for the material of interest. This chemical speciation fingerprint (CSF) is used in subsequent chemical reaction transport modelling as a starting point. It is also a good starting point for any new sample of MSWI bottom ash, since most minerals identified here

will be relevant in such unknown samples, while the parameter settings for reactive surfaces may not be too far off.

The multi-element chemical speciation modelling is complex, but still proves very feasible as the run-time is mostly within two minutes. In the speciation modelling the outcome of the model result is optimized by iteration by applying changes in the mineral assemblage. A preliminary model run using saturation indices is used for guidance in this process. As simultaneously a model run at L/S=10 and L/S around 0.2 is carried out with the same mineral set and the same sorption properties, a good match for a wide spectrum of major, minor and trace elements is an indication that a converging solution is approached. Multiple interactions take place, implying that absolutely wrong choices of a mineral or a sorption property will show as a significant deviation from the actual measurement. As the modelling assumes equilibrium and it is certain that in the test equilibrium is not fully reached, in some cases a difference between model and measurement cannot be resolved. Such cases can only be recognized by running tests at different contact times. In the work by Dijkstra *et al.* (2006) this influence of kinetics has been clearly demonstrated. In other cases the stability constants may not be well defined. This is particularly the case for some less common trace elements like Sb, V and Mo. In comparison with the total Zn content of MBA UK1 and MBA UK2 of 2514 and 1963 mg/kg, the maximum fraction available for leaching amounts to respectively 1233 and 1323 mg/kg[3].

To assess the question in what chemical form Zn is present in MSWI bottom ash, the optimized model description has been used as basis to select other Zn minerals than the ones optimally describing the release behaviour. This implies running the model with respectively, ZnO, Cazincate, $Zn(OH)_2$, Willemite ($ZnSiO_4$), $Ca_4Zn(PO_4)_3OH$,d $ZnCl_2$ and Bianchite ($Zn_{0.75}Fe^{2+}_{0.25}(SO_4)\bullet 6(H_2O)$).

Since the full description matches with the measured concentrations of major, minor and trace elements for both ashes quite well, this indicates that the complex mixture is rather well described. The description of Zn matches quite good for either $ZnSiO_3$ or $Ca_4Zn(PO_4)_3OH$. The other phases - ZnO, Cazincate, $Zn(OH)_2$, Willemite ($ZnSiO_4$), $ZnCl_2$ and Bianchite ($Zn_{0.75}Fe^{2+}_{0.25}(SO_4)\bullet 6(H_2O)$) show a poor match and therefore cannot be considered to be controlling release.

[3] This is the highest concentration released during the pH dependence leaching test, in this case, at pH2.

Table D.1 Model input parameters for IBA1

Input specification							
Prediction case			**DOC/DHA data**	**pH**	**[DOC] (kg/l)**	**DHA fraction**	**[DHA] (kg/l)**
Speciation session	WRc MBA 2011			1.00	9.000E-05	0.20	1.800E-05
Material	MSWI Bottom ash UK 1 (P,1,1)			2.10	8.370E-05	0.20	1.674E-05
				4.05	4.380E-05	0.20	8.760E-06
Solved fraction DOC	0.2			5.60	5.620E-05	0.20	1.124E-05
Sum of pH and pe	11.00			6.90	4.780E-05	0.20	9.560E-06
L/S	10.4565	**l/kg**		8.20	4.820E-05	0.20	9.640E-06
Clay	1.000E-02	**kg/kg**		9.15	4.910E-05	0.22	1.080E-05
HFO	1.700E-03	**kg/kg**		10.65	5.025E-05	0.25	1.256E-05
SHA	4.000E-04	**kg/kg**		11.90	5.160E-05	0.28	1.445E-05
Percolation material	MSWI Bottom ash UK 1 (C,1,1)			14.00	6.000E-05	0.32	1.920E-05
Avg L/S first perc. fractions	0.3000	**l/kg**	**Polynomial coeficients**				
Reactant concentrations				**C0**	-4.586E+00		
	Reactant	**mg/kg**		**C1**	-1.501E-01		
	Ag+	not measured		**C2**	1.520E-02		
	Al+3	8.861E+03		**C3**	-3.675E-04		
	ANT	not measured		**C4**	0.000E+00		
	H3AsO4	1.507E+00		**C5**	0.000E+00		
	H3BO3	6.684E+01	**Selected Minerals**	**Most significant/Relevant**	**Other**		
	Ba+2	1.044E+01		ZnSiO3	AA_2CaO_Al2O3_8H2O[s]		
	BAA	not measured			AA_3CaO_Al2O3_6H2O[s]		
	BAP	not measured			AA_Brucite		
	BBF	not measured			AA_Calcite		
	BENZENE	not measured			AA_CaO_Al2O3_10H2O[s]		
	BGP	not measured			AA_Fe[OH]3[am]		
	BKF	not measured			AA_Fe[OH]3[microcr]		
	Br-	1.700E+01			AA_Gypsum		
	Ca+2	5.555E+04			AA_Jennite		
	Cd+2	1.886E+00			AA_Magnesite		
	CHR	not measured			AA_Portlandite		
	Cl-	4.311E+03			AA_Tobermorite-II		
	CrO4-2	1.491E+01			Al[OH]3[a]		
	Cu+2	3.526E+01			alpha-TCP		
	H2CO3	1.090E+04			Ba[SCr]O4[77%SO4]		
	EOX	not measured			BaSrSO4[50%Ba]		
	ETHYLBENZENE	not measured			Ca3[AsO4]2:6H2O		
	F-	3.600E-01			Ca4Cd[PO4]3Cl		
	Fe+3	6.096E+03			Ca4Cd[PO4]3OH		
	FLA	not measured			CaCrO4		
	FLT	not measured			CaSeO4:2H2O		
	Hg+2	3.543E-05			Cd[OH]2[C]		
	I-	not measured			Cr[OH]3[C]		
	K+	2.528E+03			CuCO3[s]		
	Li+	5.029E+00			Fe_Vanadate		
	Mg+2	5.425E+03			Fe2[MoO4]3[1]		
	MIN_OIL	not measured			Fluorite		
	Mn+2	2.462E+02			Laumontite		
	MoO4-2	7.897E-01			Manganite		
	Na+	1.564E+03			Mg3[PO4]2:22H2O[c]		
	NAP	not measured			MgKPO4:6H2O[c]		
	NH4+	not measured			Ni[OH]2[s]		
	Ni+2	2.365E+01			Pb[OH]2[C]		
	NO3-	not measured			Pb2V2O7		
	PAH_EPA	not measured			Pb3[VO4]2		
	Pb+2	2.022E+02			PbCrO4		
	PHE	not measured			PbMoO4[c]		
	PO4-3	5.711E+03			Rhodochrosite		
	PYR	not measured			Sb[OH]3[s]		
	Sb[OH]6-	7.594E+00			Strengite		
	SeO4-2	7.580E-01			Strontianite		
	H4SiO4	1.180E+04			Wairakite		
	SO4-2	1.071E+04			Willemite		
	Sr+2	1.151E+02					
	Th+4	not measured					
	TOLUENE	not measured					
	UO2+	not measured					
	VO2+	2.277E+01					
	VOX	not measured					
	Zn+2	1.233E+03					

Table D.2 Model input parameters for IBA2

Input specification							
Prediction case			**DOC/DHA data**	**pH**	**[DOC] (kg/l)**	**DHA fraction**	**[DHA] (kg/l)**
Speciation session	WRc MBA 2011			1.00	4.000E-04	0.20	8.000E-05
Material	MSWI Bottom ash UK 2 (P,1,1)			2.10	3.517E-04	0.20	7.034E-05
				4.15	1.704E-04	0.20	3.408E-05
Solved fraction DOC	0.2			5.60	1.591E-04	0.20	3.182E-05
Sum of pH and pe	12.00			7.10	2.126E-04	0.20	4.252E-05
L/S	10.0000	**l/kg**		8.15	2.142E-04	0.20	4.284E-05
Clay	1.000E-02	**kg/kg**		9.10	2.124E-04	0.20	4.248E-05
HFO	1.000E-03	**kg/kg**		10.65	1.802E-04	0.20	3.604E-05
SHA	1.000E-03	**kg/kg**		11.90	1.346E-04	0.20	2.692E-05
Percolation material	MSWI Bottom ash UK 2(C,1,1)			14.00	2.000E-04	0.20	4.000E-05
Avg L/S first perc. fractions	0.3000	**l/kg**	**Polynomial coeficients**				
Reactant concentrations				**C0**	-3.656E+00		
	Reactant	**mg/kg**		**C1**	-4.726E-01		
	Ag+	not measured		**C2**	1.022E-01		
	Al+3	1.226E+04		**C3**	-9.066E-03		
	ANT	not measured		**C4**	2.784E-04		
	H3AsO4	1.583E+00		**C5**	0.000E+00		
	H3BO3	5.035E+01	**Selected Minerals**	**Most significant/Relevant**	**Other**		
	Ba+2	1.175E+01		ZnSiO3	AA_2CaO_Al2O3_8H2O[s]		
	BAA	not measured			AA_3CaO_Al2O3_6H2O[s]		
	BAP	not measured			AA_Brucite		
	BBF	not measured			AA_Calcite		
	BENZENE	not measured			AA_CaO_Al2O3_10H2O[s]		
	BGP	not measured			AA_Fe[OH]3[am]		
	BKF	not measured			AA_Fe[OH]3[microcr]		
	Br-	5.590E+01			AA_Gypsum		
	Ca+2	7.812E+04			AA_Jennite		
	Cd+2	3.222E+00			AA_Magnesite		
	CHR	not measured			AA_Portlandite		
	Cl-	7.754E+03			AA_Tobermorite-II		
	CrO4-2	2.279E+01			Al[OH]3[a]		
	Cu+2	8.204E+01			alpha-TCP		
	H2CO3	1.500E+04			Ba[SCr]O4[77%SO4]		
	EOX	not measured			Ba[SCr]O4[96%SO4]		
	ETHYLBENZENE	not measured			BaSrSO4[50%Ba]		
	F-	6.700E-01			Ca3[AsO4]2:6H2O		
	Fe+3	5.207E+03			Ca4Cd[PO4]3OH		
	FLA	not measured			CaCrO4		
	FLT	not measured			Cd[OH]2[C]		
	Hg+2	3.620E-05			Cerrusite		
	I-	not measured			Corkite		
	K+	2.790E+03			Cotunnite		
	Li+	5.821E+00			Cr[OH]3[C]		
	Mg+2	5.341E+03			Cr2O3		
	MIN_OIL	not measured			Cr-Ettringite		
	Mn+2	2.789E+02			Laumontite		
	MoO4-2	1.163E+00			Manganite		
	Na+	5.340E+03			Mg_Vanadate		
	NAP	not measured			Mg3[PO4]2:22H2O[c]		
	NH4+	not measured			MgKPO4:6H2O[c]		
	Ni+2	5.623E+01			Morenosite		
	NO3-	not measured			Ni[OH]2[s]		
	PAH_EPA	not measured			Pb[OH]2[C]		
	Pb+2	1.198E+02			Pb2O3		
	PHE	not measured			Pb2V2O7		
	PO4-3	8.527E+03			Pb3[VO4]2		
	PYR	not measured			PbCrO4		
	Sb[OH]6-	1.187E+01			PbMoO4[c]		
	SeO4-2	5.608E-01			PbO:0.3H2O		
	H4SiO4	1.449E+04			Plattnerite		
	SO4-2	1.404E+04			Rhodochrosite		
	Sr+2	1.509E+02			Strengite		
	Th+4	not measured			Strontianite		
	TOLUENE	not measured			Wairakite		
	UO2+	not measured			Zn[OH]2[A]		
	VO2+	1.250E+01					
	VOX	not measured					
	Zn+2	1.323E+03					

Potentially ecotoxic forms such as ZnO, $ZnCl_2$ or $ZnSO_4$ would be converted in less soluble silicates or phosphates. However, the transformation rates for $ZnCl_2$, $ZnSO_4$ or $Zn(OH)_2$ are very fast because of their high solubility. Silicates and phosphates are abundantly present, so the transformation to these less critical phases is quite rapid, as any testing of bottom ash

fresh or aged shows the same solubility control. The presence of these more soluble phases in a MSWI bottom ash matrix is thus highly unlikely.

Since the full description matches with the measured concentrations of major, minor and trace elements for both ashes quite well, this indicates that the complex mixture is rather well described. The description of Zn matches quite well for either $ZnSiO_3$ or $Ca_4Zn(PO_4)_3OH$. The other phases - ZnO, Cazincate, $Zn(OH)_2$, Willemite ($ZnSiO_4$), $ZnCl_2$ and Bianchite ($Zn_{0.75}Fe^{2+}_{0.25}(SO_4)\bullet 6(H_2O)$) show a poor match with the measured concentrations i.e. undersaturation with respect to the tested phases. This implies that the latter phases are not relevant from a leaching perspective over the pH range of relevance to MSWI bottom ash in normal exposure conditions. In the field these are defined by the initial pH of the bottom ash (around pH 12) and a full carbonated bottom ash (pH around 7.5). The fraction available for leaching is a quantity that under any field exposure scenario is very unlikely to be released. On the exposed surfaces of particles, Zn will be present as $ZnSiO_3$ or $Ca_4Zn(PO_4)_3OH$ solubility control by these phases over a wide pH domain. A small part of the leachable Zn fraction is associated with DOC and may be leached. Zn-DOC is less readily available for organisms than free Zn^{2+}. The fraction of Zn-DOC is relatively small.

References

CEN/TS 14405 (2004): Characterization of waste - Leaching behaviour tests - Up-flow percolation test (under specified conditions), CEN, Brussels, Belgium.

CEN/TS 14429 (2005). Characterization of waste - Leaching behaviour tests - Influence of pH on leaching with initial acid/base addition, CEN, Brussels, Belgium.

CEN/TS 14997 (2005). Characterization of waste - Leaching behaviour tests - Influence of pH on leaching with continuous pH control. CEN/TC292.

Dijkstra, J.J., van der Sloot, H.A. and Comans, R.N.J. (2006). The leaching of major and trace elements from MSWI bottom ash as a function of pH and time, Appl. Geochem. 21, 335-351.

Dzombak, D.A. and Morel, F.M.M. (1990). Surface complexation modelling: hydrous ferric oxide, John Wiley & Sons, Inc., New York.

ISO/TS 21268-3, Soil quality - Leaching procedures for subsequent chemical and ecotoxicological testing of soil and soil materials - Part 3: Up-flow column test, ISO. 2007.

ISO/TS 21268-4, Soil quality - Leaching procedures for subsequent chemical and ecotoxicological testing of soil and soil materials - Part 4: Influence of pH on leaching with initial acid/base addition, ISO. 2007.

ISO/DIS12782 parts 1-5 (2010) Soil quality - Parameters for geochemical modelling of leaching and speciation of constituents in soils and soil materials - Part 1: Extraction of amorphous iron (hydr)oxides with ascorbic acid; Part 2: Extraction of crystalline iron (hydr)oxides with dithionite; Part 3: Extraction of aluminium (hydr)oxides with ammonium oxalate - oxalic acid; Part 4: Extraction of humic substances from solid samples. Part 5: Extraction of humic substances from aqueous samples. ISO, Geneve, Switzerland.

Kinniburgh, D.G., van Riemsdijk, W.H., Koopal, L.K., Borkovec, M., Benedetti, M.F. and Avena, M.J. (1999). Ion binding to natural organic matter: competition, heterogeneity, stoichiometry and thermodynamic consistency, J. Colloids Surf., A, Vol. 151, pp. 147-166.

Kostka, J.E. and Luther III, G.W. (1994). "Partitioning and speciation of solid phase iron in saltmarsh sediments", Geochim. Cosmochim. Acta, 58, 1701-1710.

LeachXS Lite - http://www.vanderbilt.edu/leaching/downloads.html

Meeussen, J.C.L. (2003). "ORCHESTRA: An object-oriented framework for implementing chemical equilibrium models", Environ. Sci. Technol., 37, 1175-1182.

Meima, J.A. and Comans, R.N.J. (1998). Application of surface complexation/precipitation modelling to contaminant leaching from weathered municipal solid waste incinerator bottom ash, Environ. Sci. Technol., 32, 688-693.

Milne, C.J., Kinniburgh, D.G., van Riemsdijk, W.H. and Tipping, E. (2003). Generic NICA-Donnan model parameters for metal-ion binding by humic substances, Environ. Sci. Technol., Vol. 37, pp. 958-971.

Garrabrants, A.C., Kosson, D.S., van der Sloot, H.A., Sanchez, F. and Hjelmar, O. 2010. "Background Information for the Leaching Environmental Assessment Framework (LEAF) Test Methods" USEPA, EPA/600/R-10/170.Preliminary EPA Method 1313 (2009) - Leaching test (liquid-solid partitioning as a function of extract ph) of inorganic species in solid materials using a parallel batch.

van der Sloot (2001) Integration of lab-scale testing, lysimeter studies and pilot scale monitoring of a predominantly inorganic waste landfill to reach sustainable landfill conditions, Conference Proceeding, van der Sloot, H.A. van Zomeren, A. Rietra, R.P.J.J. Hoede, D. Scharff, H. Pula, Cagliari, Italy CISA - Environmental Sanitary Engineering Centre, Eighth International waste management and landfill symposium.

van der Sloot. (2003) Evaluation of environmental aspects of alternative materials using an integrated approach assisted by a database, Conference Proceeding, van der Sloot, H.A. Seignette, P. Comans, R.N.J. van Dijkstra, J.J. Meeussen, J.C.L. Kosson, D.S. Hjelmar, O. 2003769790, University of Dundee, Dundee, Scotland, Conference on advances in waste management and recycling.

van der Sloot. (2007) Interpretation of test method selection, validation against field data, and predictive modelling for impact evaluation of stabilised waste disposal, Journal, van der Sloot, H.A. van Zomeren, A. Meeussen, J.C.L. Seignette, P. Bleijerveld, Journal of Hazardous Materials.

van der Sloot. (2008) Characterisation of waste through leaching and geochemical modelling to evaluate reuse potential, treatment options and disposal, van der Sloot, H.A. Hjelmar, O. Kosson, D.S. 2007 S. Margherita di Pula, Cagliari, Italy CISA - Environmental Sanitary Engineering Centre, Cagliari, Italy 11th international waste management and landfill symposium.

Appendix E Interpretation of Leaching Test Data

The following series of plots shows the leaching test data for the UK IBA1 sample on the left and UK IBA 2 sample on the right. Data from the pH dependence test are shown by the red dots, and the upflow percolation test data shown by the blue dots. The concentration leached in mol/l is shown on the y-axis (on a log scale) and the pH at which the leaching was undertaken is shown on the x-axis. The upflow percolation test is carried out at the pH of the substance examined at a series of increasing liquid:solid ratios.

The red dashed line shows the model description on the basis of the liquid solid ratio at which the pH dependence test is carried out (L/S = 10) and the blue dashed line shows the model prediction at lower liquid solid ratios more likely to prevail in the environment (L/S ratio = 0.3). Red dots are the measured pH dependence test data and the blue dots are the percolation test data plotted at the pH observed in the respective fractions. Predicted release is modelled on the basis of:

- Mineral precipitation
- Iron oxide and aluminium oxide sorption
- Clay interaction
- Particulate interaction
- Dissolved organic carbon

For example, for the $ZnSiO_3$ plot (Figure 3.1), the leaching data shows very good agreement with the model, in that the predicted pH dependence of the observed leaching matches that which is predicted. The zinc release is controlled by this form.

The model for ZnO (an ecotoxic phase) shows very poor agreement for both samples (e.g. Figure 3.2). The model for this zinc species predicts much higher zinc leachability (particularly between pH 7-12) than what is observed and is therefore a very poor match. This would indicate that zinc would be present as ZnO, it would be readily converted to less soluble forms.

A similarly poor fit was obtained for ZnO, cazincate, $Zn(OH)_2$, willemite ($ZnSiO_4$), $ZnCl_2$ and bianchite ($Zn_{0.75}Fe^{2+}_{0.25}(SO_4)\cdot 6(H_2O)$). This implies that the latter phases are not the phases controlling leaching over the pH range of relevance to IBA in normal exposure conditions, or in fresh ash as it leaves the facility. Any soluble zinc will dissolve and more or less immediately re-precipitate as the less soluble silicates and phosphates – as would happen when the ash is quenched as it comes out of the boiler.

Appendix F Plots from Geochemical Modelling – UK and Worldwide Data

Appendix F1 Multielement geochemical modelling of MSWI bottom ashes from different sources with the emphasis on Zn solubility controlling phases

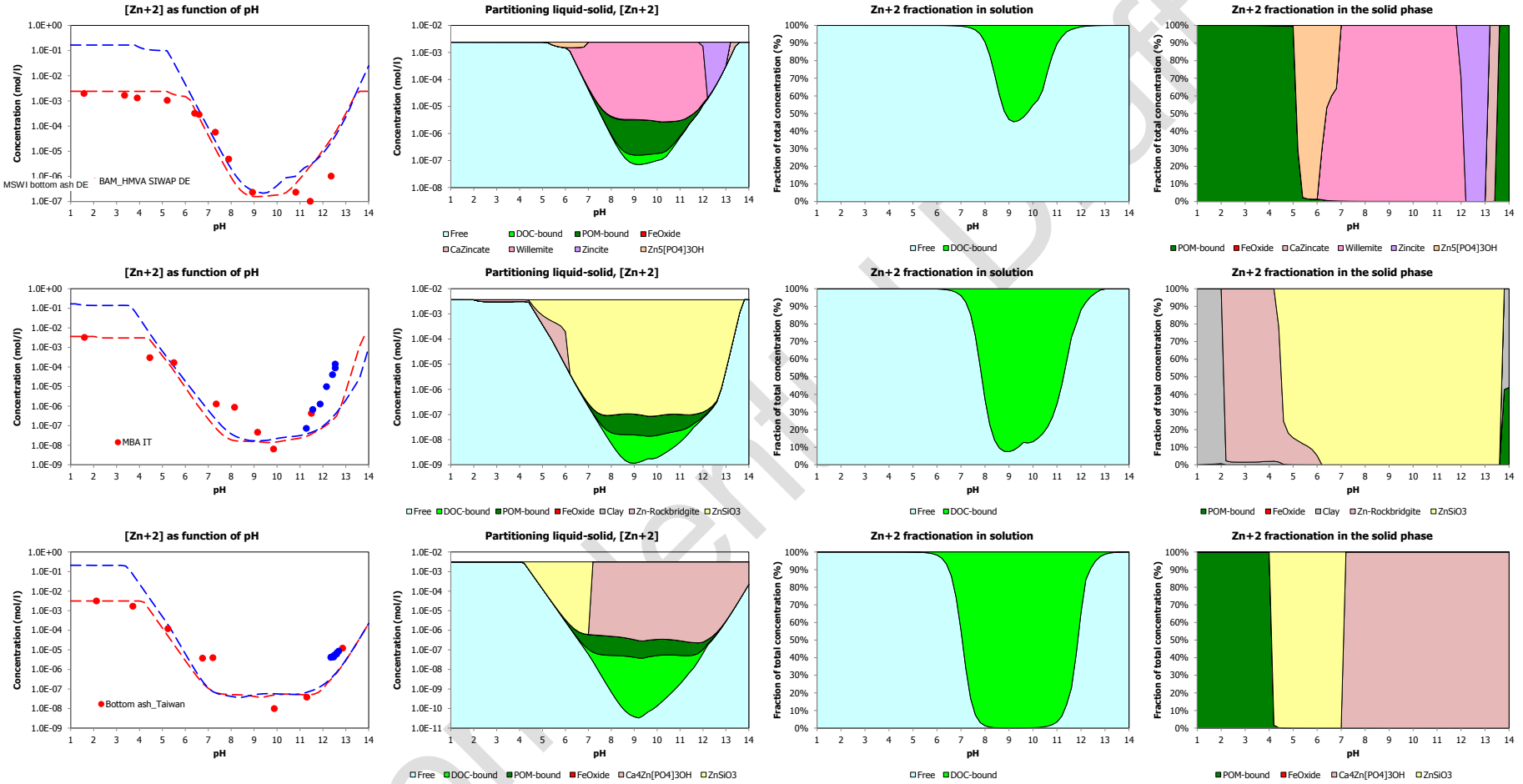

Figure F.1 Geochemical modelling of Zn release from IBA from Germany, Italy and Taiwan including partitioning between dissolved and solid phases
Legend for left figure: red dots – pH dependence test data at L/S=10 mL/g; blue triangles – column test data ranging from L/S 0.1 to 10 mL/g; red broken line – model description for L/S=10 mL/g; dotted line – model prediction for L/S=0.3 mL/g. One to the right: partitioning in solid and in solution (Mol/L basis). Next two graphs: partitioning in solution and in the solid phase (percent)

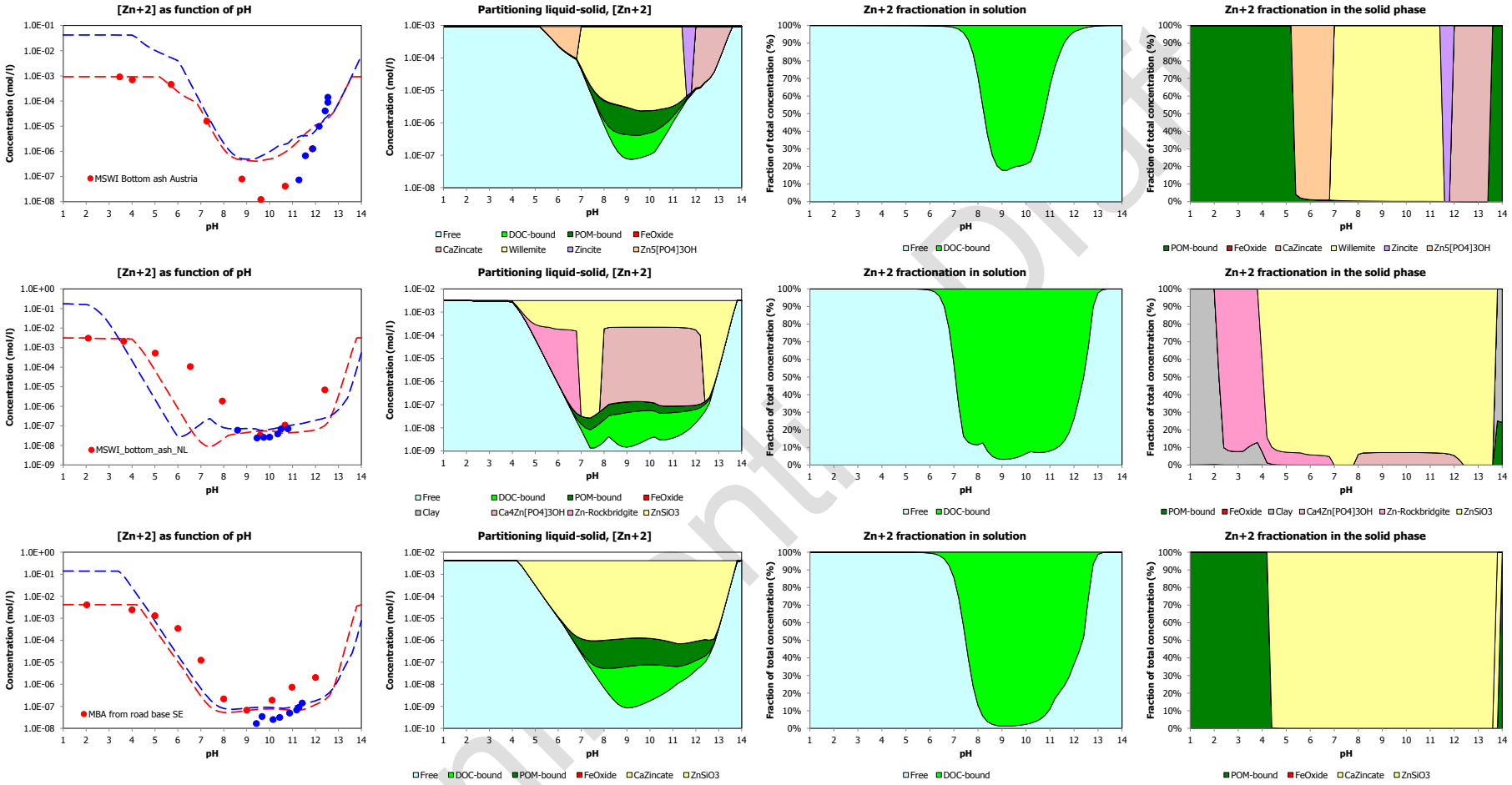

Figure F.2 Geochemical modelling of Zn release from IBAs from Austria, Netherlands and Sweden including partitioning between dissolved and solid phases

Legend for left figure: red dots – pH dependence test data at L/S=10 mL/g; blue triangles – column test data ranging from L/S 0.1 to 10 mL/g; red broken line – model description for L/S=10 mL/g; dotted line – model prediction for L/S=0.3 mL/g. One to the right: partitioning in solid and in solution (Mol/L basis). Next two graphs: partitioning in solution and in the solid phase (percent)

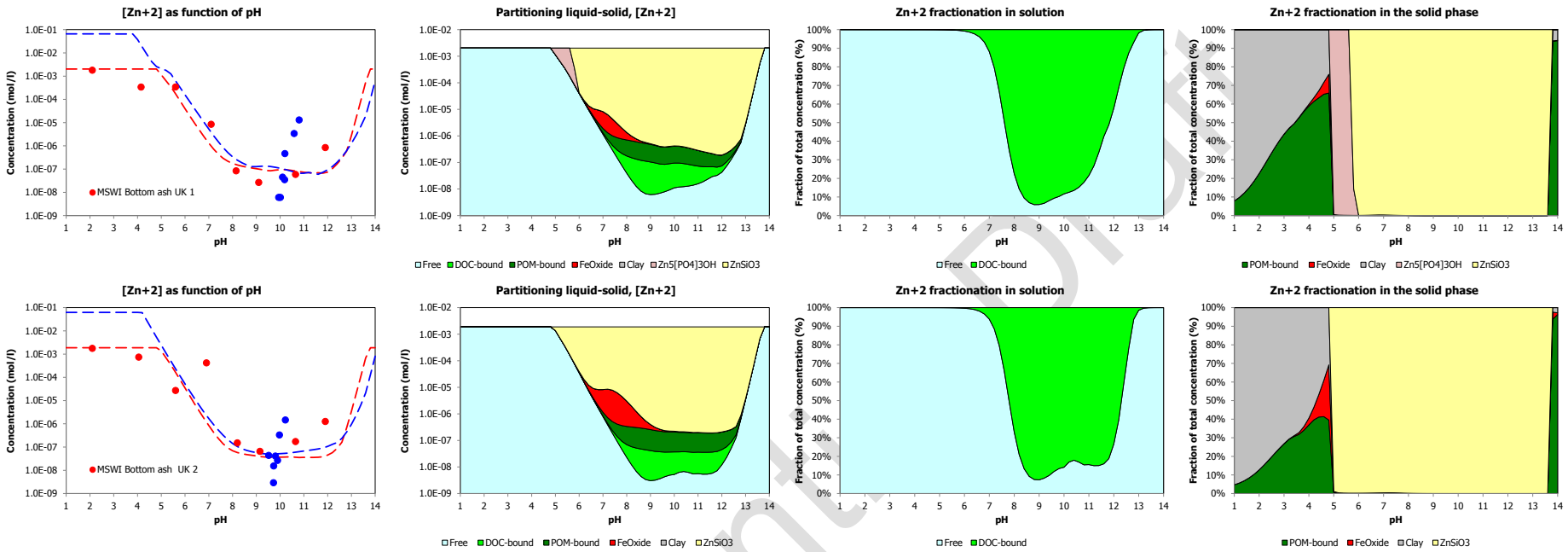

Figure F.3 Geochemical modelling of Zn release from fresh IBA from UK including partitioning between dissolved and solid phases

Legend for left figure: red dots – pH dependence test data at L/S=10 mL/g; blue triangles – column test data ranging from L/S 0.1 to 10 mL/g; red broken line – model description for L/S=10 mL/g; dotted line – model prediction for L/S=0.3 mL/g. One to the right: partitioning in solid and in solution (Mol/L basis). Next two graphs: partitioning in solution and in the solid phase (percent)

Appendix F2 – zinc solid phase fractionation plots only

UKIBA1 Fresh ESA sample 1

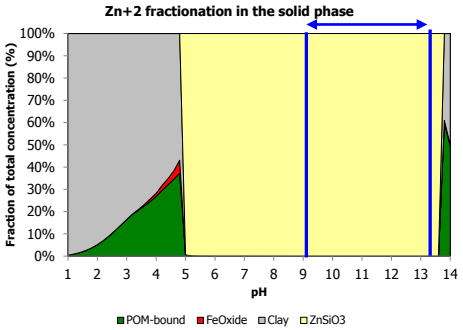

UKIBA2 Fresh ESA sample 2

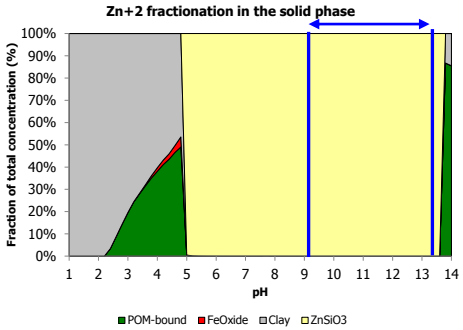

UK3 – Aged UK IBA

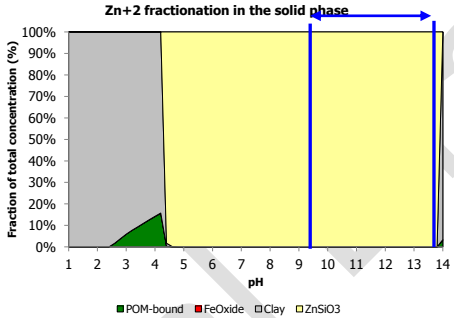

UK4 – Aged UK IBA

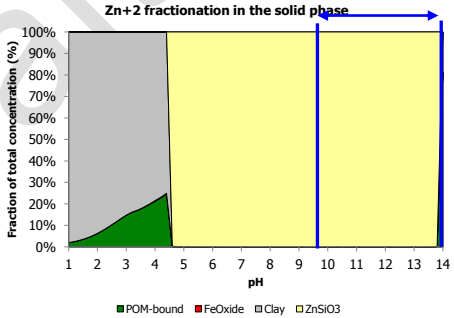

UK5 – Aged UK IBA

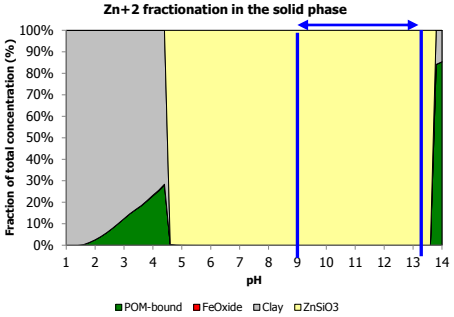

UK6 – Aged UK IBA

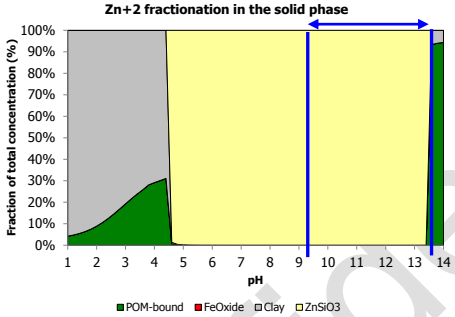

UK7 – Aged UK IBA

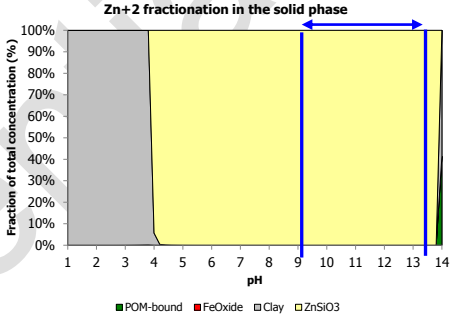

Germany

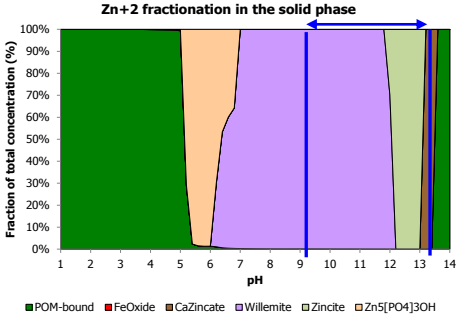

Austria

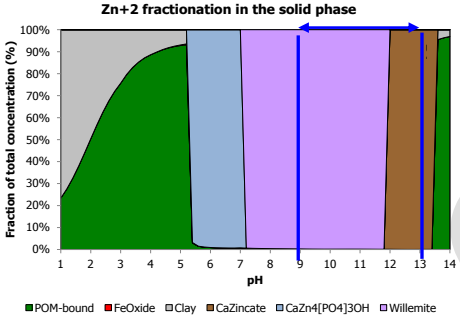

Netherlands 1

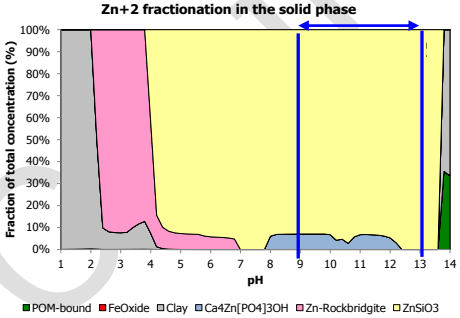

Netherlands 2

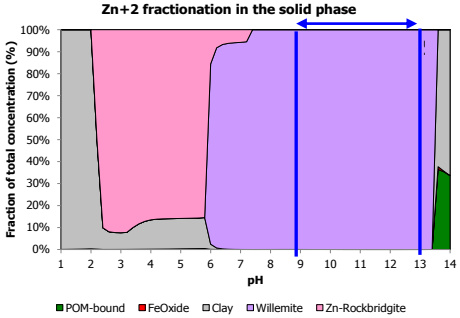

Taiwan

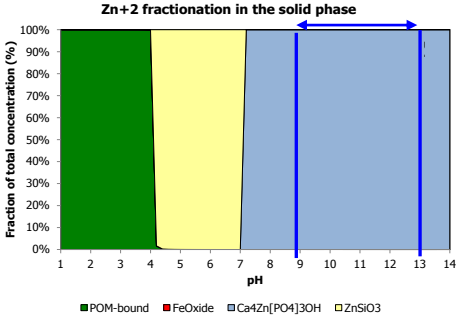

Appendix F3 – copper solid phase fractionation plots only

UKIBA1 Fresh ESA sample 1

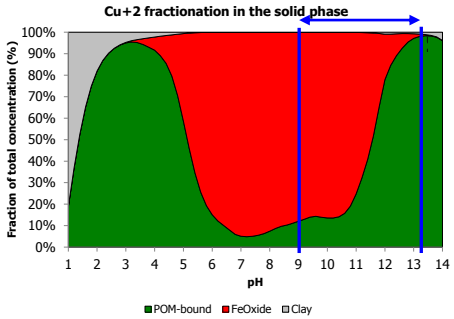

UKIBA2 Fresh ESA sample 2

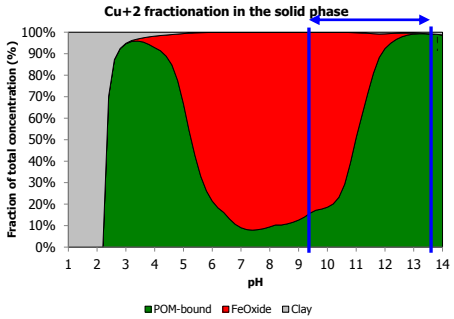

UK3 – Aged UK IBA

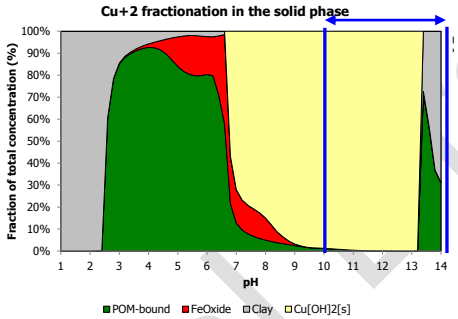

UK4 – Aged UK IBA

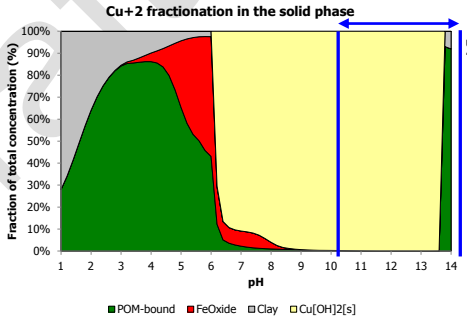

UK5 – Aged UK IBA

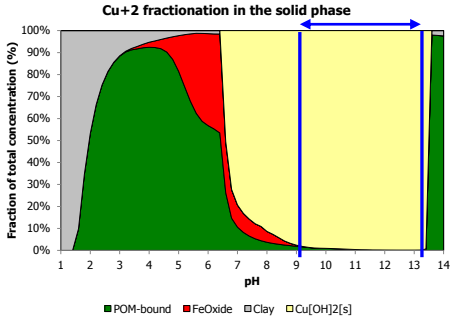

UK6 – Aged UK IBA

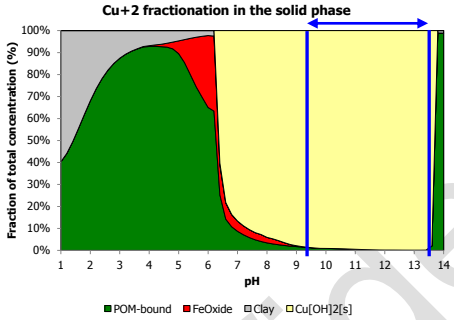

UK7 – Aged UK IBA

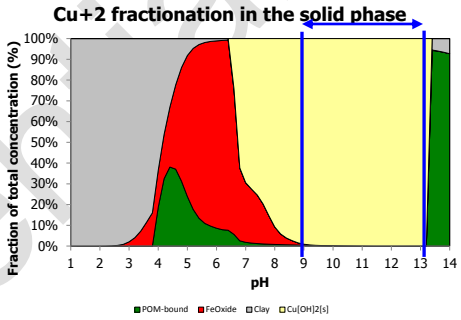

Germany

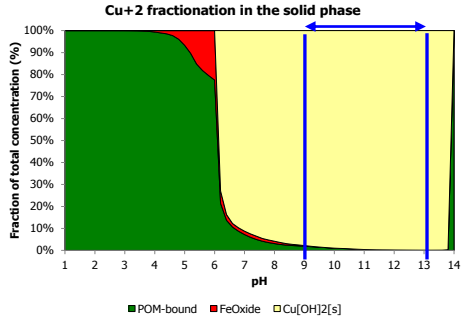

Austria

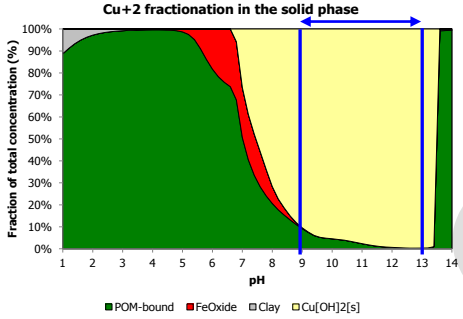

Netherlands 1

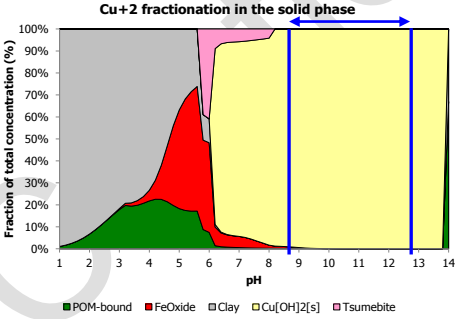

Netherlands 2

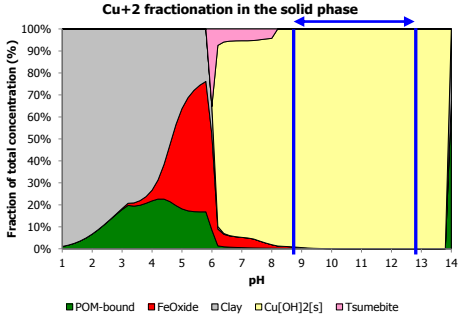

Taiwan

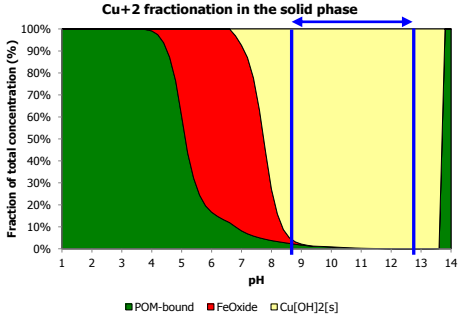

Appendix F4 – copper model input parameters

Input specification							
Prediction case			**DOC/DHA data**	**pH**	**[DOC] (kg/l)**	**DHA fraction**	**[DHA] (kg/l)**
Speciation session	WRc MBA 2011			1.00	9.000E-05	0.20	1.800E-05
Material	MSWI Bottom ash UK 1 (P,1,1)			2.10	8.370E-05	0.20	1.674E-05
				4.05	4.380E-05	0.20	8.760E-06
Solved fraction DOC	0.2			5.60	5.620E-05	0.20	1.124E-05
Sum of pH and pe	11.00			6.90	4.780E-05	0.20	9.560E-06
L/S	10.4565	**l/kg**		8.20	4.820E-05	0.20	9.640E-06
Clay	1.000E-02	**kg/kg**		9.15	4.910E-05	0.22	1.080E-05
HFO	1.700E-03	**kg/kg**		10.65	5.025E-05	0.25	1.256E-05
SHA	4.000E-04	**kg/kg**		11.90	5.160E-05	0.28	1.445E-05
Percolation material	MSWI Bottom ash UK 1 (C,1,1)			14.00	6.000E-05	0.32	1.920E-05
Avg L/S first perc. fractions	0.3000	**l/kg**	**Polynomial coeficients**				
Reactant concentrations				**C0**	-4.586E+00		
	Reactant	**mg/kg**		**C1**	-1.501E-01		
	Ag+	not measured		**C2**	1.520E-02		
	Al+3	8.861E+03		**C3**	-3.675E-04		
	ANT	not measured		**C4**	0.000E+00		
	H3AsO4	1.507E+00		**C5**	0.000E+00		
	H3BO3	6.684E+01	**Selected Minerals**	**Most significant/Relevant**	**Other**		
	Ba+2	1.044E+01			AA_2CaO_Al2O3_8H2O[s]		
	BAA	not measured			AA_3CaO_Al2O3_6H2O[s]		
	BAP	not measured			AA_Brucite		
	BBF	not measured			AA_Calcite		
	BENZENE	not measured			AA_CaO_Al2O3_10H2O[s]		
	BGP	not measured			AA_Fe[OH]3[am]		
	BKF	not measured			AA_Fe[OH]3[microcr]		
	Br-	1.700E+01			AA_Gypsum		
	Ca+2	5.555E+04			AA_Jennite		
	Cd+2	1.886E+00			AA_Magnesite		
	CHR	not measured			AA_Portlandite		
	Cl-	4.311E+03			AA_Tobermorite-II		
	CrO4-2	1.491E+01			Al[OH]3[a]		
	Cu+2	3.526E+01			alpha-TCP		
	H2CO3	1.090E+04			Ba[SCr]O4[77%SO4]		
	EOX	not measured			BaSrSO4[50%Ba]		
	ETHYLBENZENE	not measured			Ca3[AsO4]2:6H2O		
	F-	3.600E-01			Ca4Cd[PO4]3Cl		
	Fe+3	6.096E+03			Ca4Cd[PO4]3OH		
	FLA	not measured			CaCrO4		
	FLT	not measured			CaSeO4:2H2O		
	Hg+2	3.543E-05			Cd[OH]2[C]		
	I-	not measured			Cr[OH]3[C]		
	K+	2.528E+03			CuCO3[s]		
	Li+	5.029E+00			Fe_Vanadate		
	Mg+2	5.425E+03			Fe2[MoO4]3[1]		
	MIN_OIL	not measured			Fluorite		
	Mn+2	2.462E+02			Laumontite		
	MoO4-2	7.897E-01			Manganite		
	Na+	1.564E+03			Mg3[PO4]2:22H2O[c]		
	NAP	not measured			MgKPO4:6H2O[c]		
	NH4+	not measured			Ni[OH]2[s]		
	Ni+2	2.365E+01			Pb[OH]2[C]		
	NO3-	not measured			Pb2V2O7		
	PAH_EPA	not measured			Pb3[VO4]2		
	Pb+2	2.022E+02			PbCrO4		
	PHE	not measured			PbMoO4[c]		
	PO4-3	5.711E+03			Rhodochrosite		
	PYR	not measured			Sb[OH]3[s]		
	Sb[OH]6-	7.594E+00			Strengite		
	SeO4-2	7.580E-01			Strontianite		
	H4SiO4	1.180E+04			Wairakite		
	SO4-2	1.071E+04			Willemite		
	Sr+2	1.151E+02			ZnSiO3		
	Th+4	not measured					
	TOLUENE	not measured					
	UO2+	not measured					
	VO2+	2.277E+01					
	VOX	not measured					
	Zn+2	1.233E+03					

Input specification							
Prediction case			**DOC/DHA data**	**pH**	**[DOC] (kg/l)**	**DHA fraction**	**[DHA] (kg/l)**
Speciation session	WRc MBA 2011			1.00	4.000E-04	0.20	8.000E-05
Material	MSWI Bottom ash UK 2 (P,1,1)			2.10	3.517E-04	0.20	7.034E-05
				4.15	1.704E-04	0.20	3.408E-05
Solved fraction DOC	0.2			5.60	1.591E-04	0.20	3.182E-05
Sum of pH and pe	12.00			7.10	2.126E-04	0.20	4.252E-05
L/S	10.0000	**l/kg**		8.15	2.142E-04	0.20	4.284E-05
Clay	1.000E-02	**kg/kg**		9.10	2.124E-04	0.20	4.248E-05
HFO	1.000E-03	**kg/kg**		10.65	1.802E-04	0.20	3.604E-05
SHA	1.000E-03	**kg/kg**		11.90	1.346E-04	0.20	2.692E-05
Percolation material	MSWI Bottom ash UK 2 (C,1,1)			14.00	2.000E-04	0.20	4.000E-05
Avg L/S first perc. fractions	0.3000	**l/kg**	**Polynomial coeficients**				
Reactant concentrations				**C0**	-3.656E+00		
	Reactant	**mg/kg**		**C1**	-4.726E-01		
	Ag+	not measured		**C2**	1.022E-01		
	Al+3	1.226E+04		**C3**	-9.066E-03		
	ANT	not measured		**C4**	2.784E-04		
	H3AsO4	1.583E+00		**C5**	0.000E+00		
	H3BO3	5.035E+01	**Selected Minerals**	**Most significant/Relevant**	**Other**		
	Ba+2	1.175E+01			AA_2CaO_Al2O3_8H2O[s]		
	BAA	not measured			AA_3CaO_Al2O3_6H2O[s]		
	BAP	not measured			AA_Brucite		
	BBF	not measured			AA_Calcite		
	BENZENE	not measured			AA_CaO_Al2O3_10H2O[s]		
	BGP	not measured			AA_Fe[OH]3[am]		
	BKF	not measured			AA_Fe[OH]3[microcr]		
	Br-	5.590E+01			AA_Gypsum		
	Ca+2	7.812E+04			AA_Jennite		
	Cd+2	3.222E+00			AA_Magnesite		
	CHR	not measured			AA_Portlandite		
	Cl-	7.754E+03			AA_Tobermorite-II		
	CrO4-2	2.279E+01			Al[OH]3[a]		
	Cu+2	8.204E+01			alpha-TCP		
	H2CO3	1.500E+04			Ba[SCr]O4[77%SO4]		
	EOX	not measured			Ba[SCr]O4[96%SO4]		
	ETHYLBENZENE	not measured			BaSrSO4[50%Ba]		
	F-	6.700E-01			Ca3[AsO4]2:6H2O		
	Fe+3	5.207E+03			Ca4Cd[PO4]3OH		
	FLA	not measured			CaCrO4		
	FLT	not measured			Cd[OH]2[C]		
	Hg+2	3.620E-05			Cerrusite		
	I-	not measured			Corkite		
	K+	2.790E+03			Cotunnite		
	Li+	5.821E+00			Cr[OH]3[C]		
	Mg+2	5.341E+03			Cr2O3		
	MIN_OIL	not measured			Cr-Ettringite		
	Mn+2	2.789E+02			Laumontite		
	MoO4-2	1.163E+00			Manganite		
	Na+	5.340E+03			Mg_Vanadate		
	NAP	not measured			Mg3[PO4]2:22H2O[c]		
	NH4+	not measured			MgKPO4:6H2O[c]		
	Ni+2	5.623E+01			Morenosite		
	NO3-	not measured			Ni[OH]2[s]		
	PAH_EPA	not measured			Pb[OH]2[C]		
	Pb+2	1.198E+02			Pb2O3		
	PHE	not measured			Pb2V2O7		
	PO4-3	8.527E+03			Pb3[VO4]2		
	PYR	not measured			PbCrO4		
	Sb[OH]6-	1.187E+01			PbMoO4[c]		
	SeO4-2	5.608E-01			PbO:0.3H2O		
	H4SiO4	1.449E+04			Plattnerite		
	SO4-2	1.404E+04			Rhodochrosite		
	Sr+2	1.509E+02			Strengite		
	Th+4	not measured			Strontianite		
	TOLUENE	not measured			Wairakite		
	UO2+	not measured			Zn[OH]2[A]		
	VO2+	1.250E+01			ZnSiO3		
	VOX	not measured					
	Zn+2	1.323E+03					

Appendix F5 – nickel solid phase fractionation plots only

UKIBA1 Fresh ESA sample 1

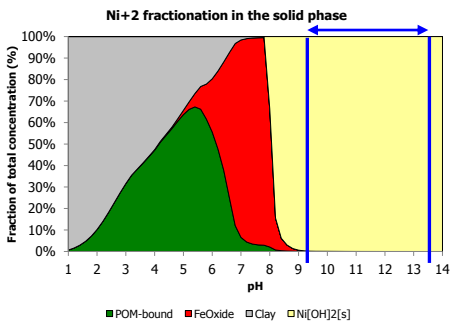

UKIBA2 Fresh ESA sample 2

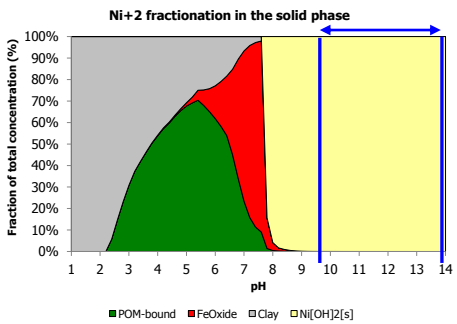

UK3 – Aged UK IBA

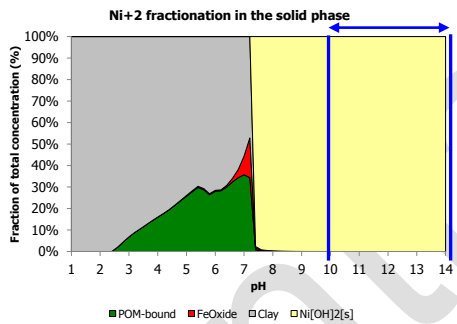

UK4 – Aged UK IBA

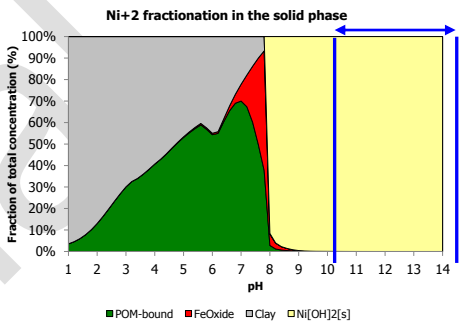

UK5 – Aged UK IBA

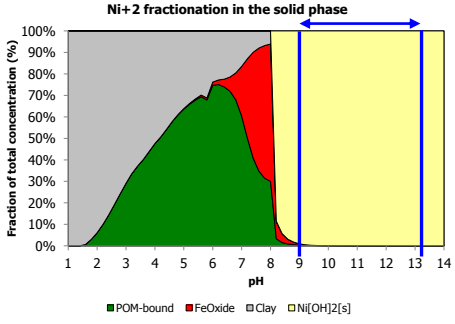

UK6 – Aged UK IBA

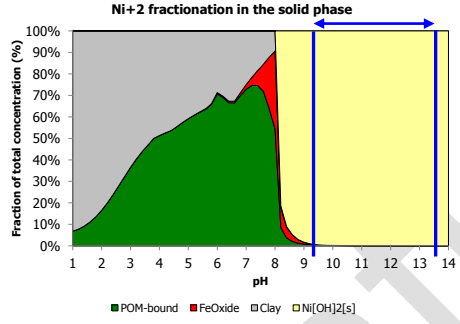

UK7 – Aged UK IBA

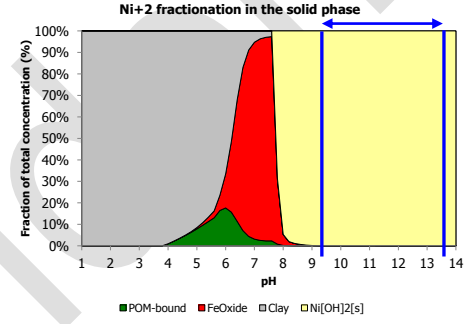

Germany

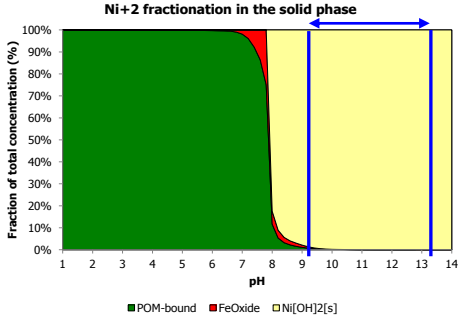

Austria

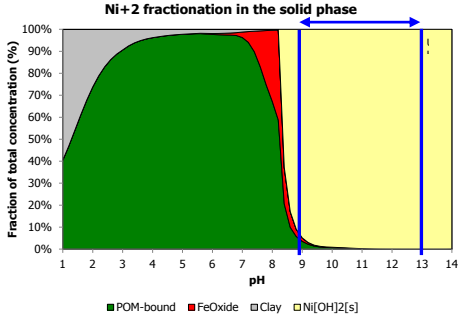

Netherlands 1

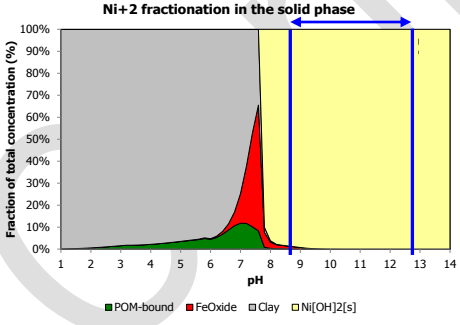

Netherlands 2

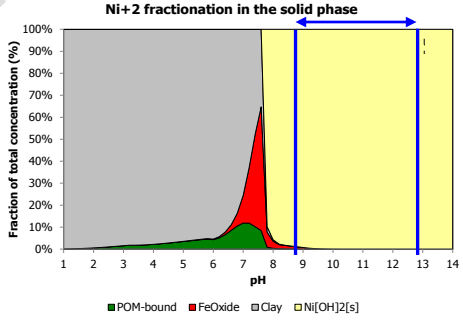

Taiwan

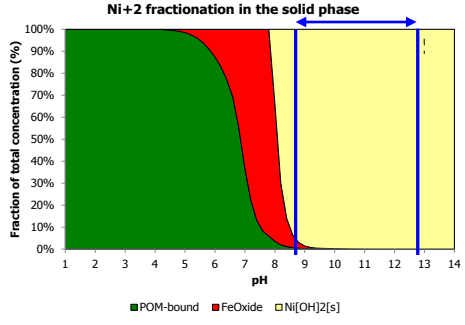

Appendix F6 – Nickel model input parameters

Input specification							
Prediction case			**DOC/DHA data**	**pH**	**[DOC] (kg/l)**	**DHA fraction**	**[DHA] (kg/l)**
Speciation session	WRc MBA 2011			1.00	9.000E-05	0.20	1.800E-05
Material	MSWI Bottom ash UK 1 (P,1,1)			2.10	8.370E-05	0.20	1.674E-05
				4.05	4.380E-05	0.20	8.760E-06
Solved fraction DOC	0.2			5.60	5.620E-05	0.20	1.124E-05
Sum of pH and pe	11.00			6.90	4.780E-05	0.20	9.560E-06
L/S	10.4565	**l/kg**		8.20	4.820E-05	0.20	9.640E-06
Clay	1.000E-02	**kg/kg**		9.15	4.910E-05	0.22	1.080E-05
HFO	1.700E-03	**kg/kg**		10.65	5.025E-05	0.25	1.256E-05
SHA	4.000E-04	**kg/kg**		11.90	5.160E-05	0.28	1.445E-05
Percolation material	MSWI Bottom ash UK 1 (C,1,1)			14.00	6.000E-05	0.32	1.920E-05
Avg L/S first perc. fractions	0.3000	**l/kg**	**Polynomial coeficients**				
Reactant concentrations				**C0**	-4.586E+00		
	Reactant	**mg/kg**		**C1**	-1.501E-01		
	Ag+	not measured		**C2**	1.520E-02		
	Al+3	8.861E+03		**C3**	-3.675E-04		
	ANT	not measured		**C4**	0.000E+00		
	H3AsO4	1.507E+00		**C5**	0.000E+00		
	H3BO3	6.684E+01	**Selected Minerals**	**Most significant/Relevant**	**Other**		
	Ba+2	1.044E+01		Ni[OH]2[s]	AA_2CaO_Al2O3_8H2O[s]		
	BAA	not measured			AA_3CaO_Al2O3_6H2O[s]		
	BAP	not measured			AA_Brucite		
	BBF	not measured			AA_Calcite		
	BENZENE	not measured			AA_CaO_Al2O3_10H2O[s]		
	BGP	not measured			AA_Fe[OH]3[am]		
	BKF	not measured			AA_Fe[OH]3[microcr]		
	Br-	1.700E+01			AA_Gypsum		
	Ca+2	5.555E+04			AA_Jennite		
	Cd+2	1.886E+00			AA_Magnesite		
	CHR	not measured			AA_Portlandite		
	Cl-	4.311E+03			AA_Tobermorite-II		
	CrO4-2	1.491E+01			Al[OH]3[a]		
	Cu+2	3.526E+01			alpha-TCP		
	H2CO3	1.090E+04			Ba[SCr]O4[77%SO4]		
	EOX	not measured			BaSrSO4[50%Ba]		
	ETHYLBENZENE	not measured			Ca3[AsO4]2:6H2O		
	F-	3.600E-01			Ca4Cd[PO4]3Cl		
	Fe+3	6.096E+03			Ca4Cd[PO4]3OH		
	FLA	not measured			CaCrO4		
	FLT	not measured			CaSeO4:2H2O		
	Hg+2	3.543E-05			Cd[OH]2[C]		
	I-	not measured			Cr[OH]3[C]		
	K+	2.528E+03			CuCO3[s]		
	Li+	5.029E+00			Fe_Vanadate		
	Mg+2	5.425E+03			Fe2[MoO4]3[1]		
	MIN_OIL	not measured			Fluorite		
	Mn+2	2.462E+02			Laumontite		
	MoO4-2	7.897E-01			Manganite		
	Na+	1.564E+03			Mg3[PO4]2:22H2O[c]		
	NAP	not measured			MgKPO4:6H2O[c]		
	NH4+	not measured			Pb[OH]2[C]		
	Ni+2	2.365E+01			Pb2V2O7		
	NO3-	not measured			Pb3[VO4]2		
	PAH_EPA	not measured			PbCrO4		
	Pb+2	2.022E+02			PbMoO4[c]		
	PHE	not measured			Rhodochrosite		
	PO4-3	5.711E+03			Sb[OH]3[s]		
	PYR	not measured			Strengite		
	Sb[OH]6-	7.594E+00			Strontianite		
	SeO4-2	7.580E-01			Wairakite		
	H4SiO4	1.180E+04			Willemite		
	SO4-2	1.071E+04			ZnSiO3		
	Sr+2	1.151E+02					
	Th+4	not measured					
	TOLUENE	not measured					
	UO2+	not measured					
	VO2+	2.277E+01					
	VOX	not measured					
	Zn+2	1.233E+03					

Input specification							
Prediction case			**DOC/DHA data**	**pH**	**[DOC] (kg/l)**	**DHA fraction**	**[DHA] (kg/l)**
Speciation session	WRc MBA 2011			1.00	4.000E-04	0.20	8.000E-05
Material	MSWI Bottom ash UK 2 (P,1,1)			2.10	3.517E-04	0.20	7.034E-05
				4.15	1.704E-04	0.20	3.408E-05
Solved fraction DOC	0.2			5.60	1.591E-04	0.20	3.182E-05
Sum of pH and pe	12.00			7.10	2.126E-04	0.20	4.252E-05
L/S	10.0000	**l/kg**		8.15	2.142E-04	0.20	4.284E-05
Clay	1.000E-02	**kg/kg**		9.10	2.124E-04	0.20	4.248E-05
HFO	1.000E-03	**kg/kg**		10.65	1.802E-04	0.20	3.604E-05
SHA	1.000E-03	**kg/kg**		11.90	1.346E-04	0.20	2.692E-05
Percolation material	MSWI Bottom ash UK 2 (C,1,1)			14.00	2.000E-04	0.20	4.000E-05
Avg L/S first perc. fractions	0.3000	**l/kg**	**Polynomial coeficients**				
				C0	-3.656E+00		
Reactant concentrations				**C1**	-4.726E-01		
	Reactant	**mg/kg**		**C2**	1.022E-01		
	Ag+	not measured		**C3**	-9.066E-03		
	Al+3	1.226E+04		**C4**	2.784E-04		
	ANT	not measured		**C5**	0.000E+00		
	H3AsO4	1.583E+00	**Selected Minerals**	**Most significant/Relevant**	**Other**		
	H3BO3	5.035E+01		Ni[OH]2[s]	AA_2CaO_Al2O3_8H2O[s]		
	Ba+2	1.175E+01			AA_3CaO_Al2O3_6H2O[s]		
	BAA	not measured			AA_Brucite		
	BAP	not measured			AA_Calcite		
	BBF	not measured			AA_CaO_Al2O3_10H2O[s]		
	BENZENE	not measured			AA_Fe[OH]3[am]		
	BGP	not measured			AA_Fe[OH]3[microcr]		
	BKF	not measured			AA_Gypsum		
	Br-	5.590E+01			AA_Jennite		
	Ca+2	7.812E+04			AA_Magnesite		
	Cd+2	3.222E+00			AA_Portlandite		
	CHR	not measured			AA_Tobermorite-II		
	Cl-	7.754E+03			Al[OH]3[a]		
	CrO4-2	2.279E+01			alpha-TCP		
	Cu+2	8.204E+01			Ba[SCr]O4[77%SO4]		
	H2CO3	1.500E+04			Ba[SCr]O4[96%SO4]		
	EOX	not measured			BaSrSO4[50%Ba]		
	ETHYLBENZENE	not measured			Ca3[AsO4]2:6H2O		
	F-	6.700E-01			Ca4Cd[PO4]3OH		
	Fe+3	5.207E+03			CaCrO4		
	FLA	not measured			Cd[OH]2[C]		
	FLT	not measured			Cerrusite		
	Hg+2	3.620E-05			Corkite		
	I-	not measured			Cotunnite		
	K+	2.790E+03			Cr[OH]3[C]		
	Li+	5.821E+00			Cr2O3		
	Mg+2	5.341E+03			Cr-Ettringite		
	MIN_OIL	not measured			Laumontite		
	Mn+2	2.789E+02			Manganite		
	MoO4-2	1.163E+00			Mg_Vanadate		
	Na+	5.340E+03			Mg3[PO4]2:22H2O[c]		
	NAP	not measured			MgKPO4:6H2O[c]		
	NH4+	not measured			Morenosite		
	Ni+2	5.623E+01			Pb[OH]2[C]		
	NO3-	not measured			Pb2O3		
	PAH_EPA	not measured			Pb2V2O7		
	Pb+2	1.198E+02			Pb3[VO4]2		
	PHE	not measured			PbCrO4		
	PO4-3	8.527E+03			PbMoO4[c]		
	PYR	not measured			PbO:0.3H2O		
	Sb[OH]6-	1.187E+01			Plattnerite		
	SeO4-2	5.608E-01			Rhodochrosite		
	H4SiO4	1.449E+04			Strengite		
	SO4-2	1.404E+04			Strontianite		
	Sr+2	1.509E+02			Wairakite		
	Th+4	not measured			Zn[OH]2[A]		
	TOLUENE	not measured			ZnSiO3		
	UO2+	not measured					
	VO2+	1.250E+01					
	VOX	not measured					
	Zn+2	1.323E+03					